

Converting NAD83 GPS Heights Into NAVD88 Elevations with LVGEOID, a Hybrid Geoid Height Model for the Long Valley Volcanic Region, California

Scientific Investigations Report 2007–5255

This page intentionally left blank

Converting NAD83 GPS Heights Into NAVD88 Elevations With LVGEOID, a Hybrid Geoid Height Model for the Long Valley Volcanic Region, California

By Maurizio Battaglia, Daniel Dzurisin, John Langbein, Jerry Svarc, and
David P. Hill

Scientific Investigations Report 2007–5255

**U.S. Department of the Interior
U.S. Geological Survey**

U.S. Department of the Interior
DIRK KEMPTHORNE, Secretary

U.S. Geological Survey
Mark D. Myers, Director

U.S. Geological Survey, Reston, Virginia: 2007

This report and any updates to it are available at:
<http://pubs.usgs.gov/sir/2007/5255/>

For product and ordering information:
World Wide Web: <http://www.usgs.gov/pubprod>
Telephone: 1-888-ASK-USGS

For more information on the USGS--the Federal source for science about the Earth, its natural and living resources, natural hazards, and the environment:
World Wide Web: <http://www.usgs.gov>
Telephone: 1-888-ASK-USGS

Any use of trade, product, or firm names is for descriptive purposes only and does not imply endorsement by the U.S. Government.

Although this report is in the public domain, permission must be secured from the individual copyright owners to reproduce any copyrighted materials contained within this report.

Suggested citation:
Battaglia, M., Dzurisin, D., Langbein, J., Svart, J. and Hill, D.P., 2007, Converting NAD83 GPS heights into NAVD88 elevations with LVGEOD, a hybrid geoid height model for the Long Valley volcanic region, California: U.S. Geological Survey Scientific Investigation Report 2007-5255, 32 p. [<http://pubs.usgs.gov/sir/2007/5255/>].

Manuscript approved for publication, November 13, 2007
Text edited by James W. Hendley II
Layout by Luis Menoyo

Contents

Abstract	1
Introduction.....	1
Comparing GPS and Leveling	4
Leveling.....	4
Helmert Orthometric Heights	5
GPS Ellipsoidal Heights.....	5
The Geoid Height Model.....	6
The Long Valley Caldera Hybrid Geoid Height Model LVGEOID	6
Conversion Surface.....	6
Summary and Conclusions.....	8
Acknowledgments.....	12
References Cited.....	12
Appendix. Geostatistical Analysis.....	13
Spatial Interpolation.....	13
Assessment of Spatial Uncertainty	14
Tables 1–5.....	16

Figures

1. Map of Long Valley volcanic region with GPS on leveled Bench Mark (GPSBM) sites and leveling routes.....	2
2. Relationship between the ellipsoid height h , orthometric height H , and geoid height N	4
3. Profiles of the measured geoid and GEOID03 along the GPS-on-Bench Mark sites in the Long Valley region	7
4. Geoid height profiles from leveling surveys in the Long Valley region.....	9
5. Map of the difference between LVGEOID and the GEOID03NGS geoid height model in the Long Valley region	10
6. Vertical deformation in the Long Valley region measured along the two leveling routes occupied in the summer of 2006	11
7. Vertical deformation at the permanent GPS site RDOM in Long Valley Caldera	12
8. Histogram of the conversion surface.....	13
9. Conversion surface variogram inferred from the 25 measured values	14
10. Histograms of the conversion surface (normal score) and the simulations	15
11. Normal score variogram inferred from the 25 measured values	15

Tables

1.	Leveling heights for the Long Valley region	17
2.	Long Valley region GPS-on-Bench Mark survey for 2006.....	22
3.	Experimental hybrid geoid height ($N+s$) for the Long Valley region.....	23
4.	Experimental conversion surface s for the Long Valley region	24
5.	Geoid heights at leveling benchmarks for the Long Valley region.....	25
6.	Ninty-five-percent bounds on intrusion source parameters	8
7.	Cross-validation of the variogram model for the conversion surface	14
8.	Cross-validation of the variogram model the normal score	15

Converting NAD83 GPS Heights Into NAVD88 Elevations With LVGEOID, a Hybrid Geoid Height Model for the Long Valley Volcanic Region, California

By Maurizio Battaglia¹, Daniel Dzurisin², John Langbein³, Jerry Svarc³, and David P. Hill³

Abstract

A GPS survey of leveling benchmarks done in Long Valley Caldera in 1999 showed that the application of the National Geodetic Survey (NGS) geoid model GEOID99 to tie GPS heights to historical leveling measurements would significantly underestimate the caldera ground deformation (known from other geodetic measurements). The NGS geoid model was able to correctly reproduce the shape of the deformation, but required a local adjustment to give a realistic estimate of the magnitude of the uplift. In summer 2006, the U.S. Geological Survey conducted a new leveling survey along two major routes crossing the Long Valley region from north to south (Hwy 395) and from east to west (Hwy 203 – Benton Crossing). At the same time, 25 leveling bench marks were occupied with dual frequency GPS receivers to provide a measurement of the ellipsoid heights. Using the heights from these two surveys, we were able to compute a precise geoid height model (LVGEOID) for the Long Valley volcanic region. Our results show that although the LVGEOID and the latest NGS GEOID03 model practically coincide in areas outside the caldera, there is a difference of up to 0.2 m between the two models within the caldera. Accounting for this difference is critical when using the geoid height model to estimate the ground deformation due to magmatic or tectonic activity in the caldera.

Introduction

The Global Positioning System (GPS) is commonly referred to as a three-dimensional positioning system, but heights obtained from GPS are typically expressed as elevations above an ellipsoidal model of the Earth, and not the

Earth's actual surface. As a result, GPS ellipsoidal heights are not directly comparable with heights above mean sea level, known as orthometric heights, determined by leveling surveys. The conversion from ellipsoid to orthometric heights requires a geoid height model that relates the local ellipsoid to the local geoid, where the geoid is the “equipotential surface” which would coincide exactly with the mean ocean surface (sea level) of the Earth. The difference between these two surfaces can be as large as 100 m in areas with strong topographic or subsurface density gradients.

A GPS survey of leveling benchmarks done in Long Valley in 1999 showed that straightforward application of the National Geodetic Survey (NGS) hybrid geoid model GEOID99 to tie GPS heights to historical leveling measurements significantly underestimated the caldera ground deformation as measured with other geodetic techniques (see Battaglia and others, 2003, for full discussion). The NGS geoid model was able to correctly reproduce the shape of the deformation, but needed a local adjustment to give a realistic estimate of the magnitude of the uplift.

In December 2003, the NGS released the new GEOID03 geoid height model (<http://www.ngs.noaa.gov/GEOID>). The GEOID03 model was developed in the same manner as GEOID99 using an underlying gravimetric geoid, USGG2003, and updated GPS ellipsoidal heights on leveled Bench Marks (GPSBMs). The conversion surface for GEOID03 was developed from 14,185 GPSBMs at a 5 arc-minute grid interval, which provided a substantial increase in the spatial coverage over GEOID99 and reduced errors due to interpolation. The fit to these same points afterwards using the derived GEOID03 model was within 0.0048 m (2σ) which is comprised of both correlated (attributable to GEOID03) and uncorrelated (GPS observation error) signals (Roman and others, 2004).

In summer 2006, the USGS conducted a new leveling survey along two major routes crossing the Long Valley region from north to south (HWY 395) and from east to west (HWY 203 – Benton Crossing). At the same time, 25 leveling bench marks were occupied with dual frequency GPS receivers to provide a measurement of the ellipsoid heights (fig. 1A). Using the heights from these two surveys we were able to (1)

¹University of Rome “La Sapienza”, Rome, Italy.

²U.S. Geological Survey, Cascades Volcano Observatory, Vancouver, WA.

³U.S. Geological Survey, Menlo Park, CA.

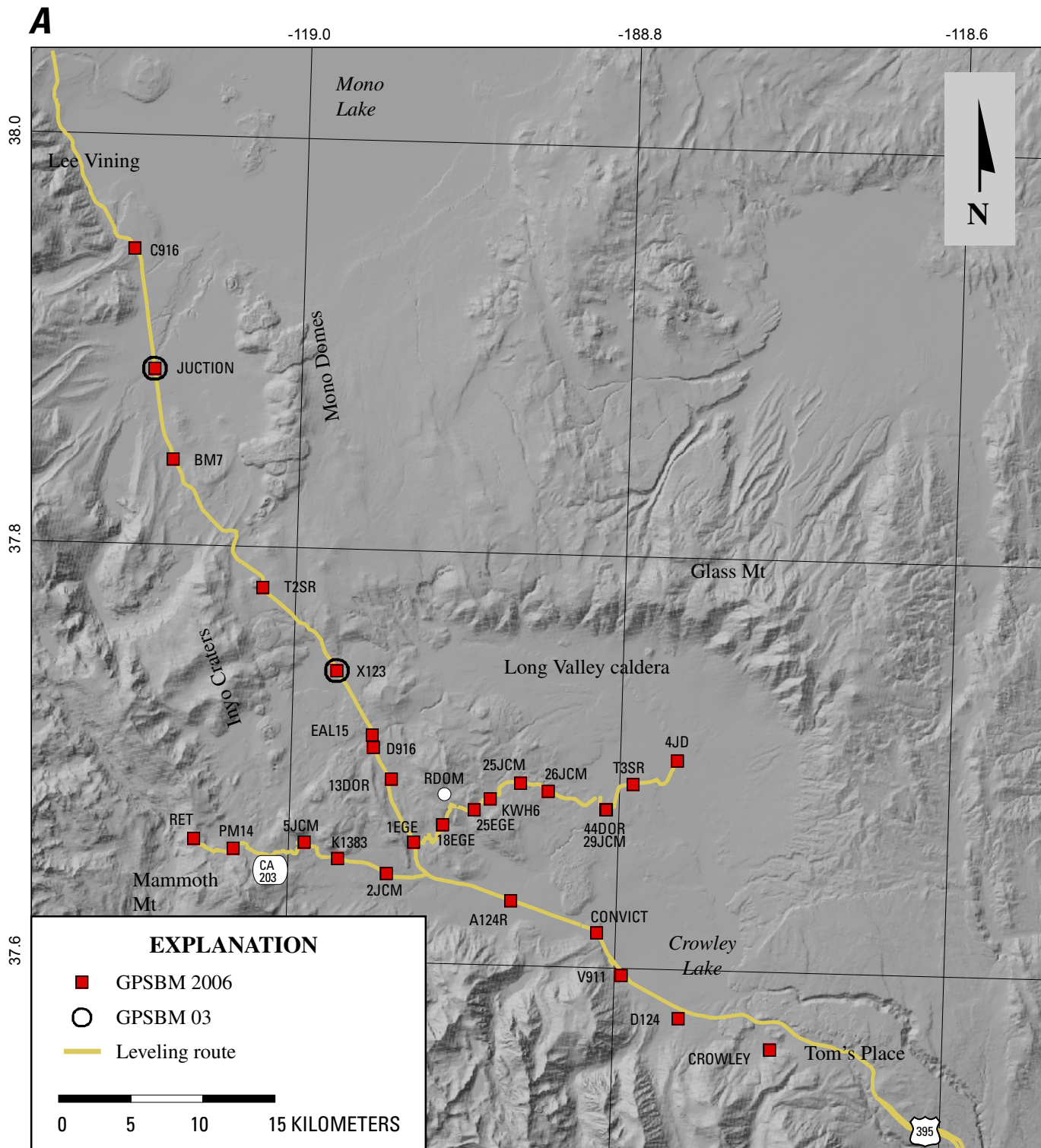


Figure 1. (A) Map of Long Valley volcanic region with GPS on leveled Bench Mark (GPSBM) sites and leveling routes. The GPSBM 03 label identifies the sites belonging to the NGS GEOID03 data base, whereas GPSBM 2006 the sites occupied by the U.S. Geological Survey in July 2006; (B) Map of Long Valley leveling routes and benchmarks.

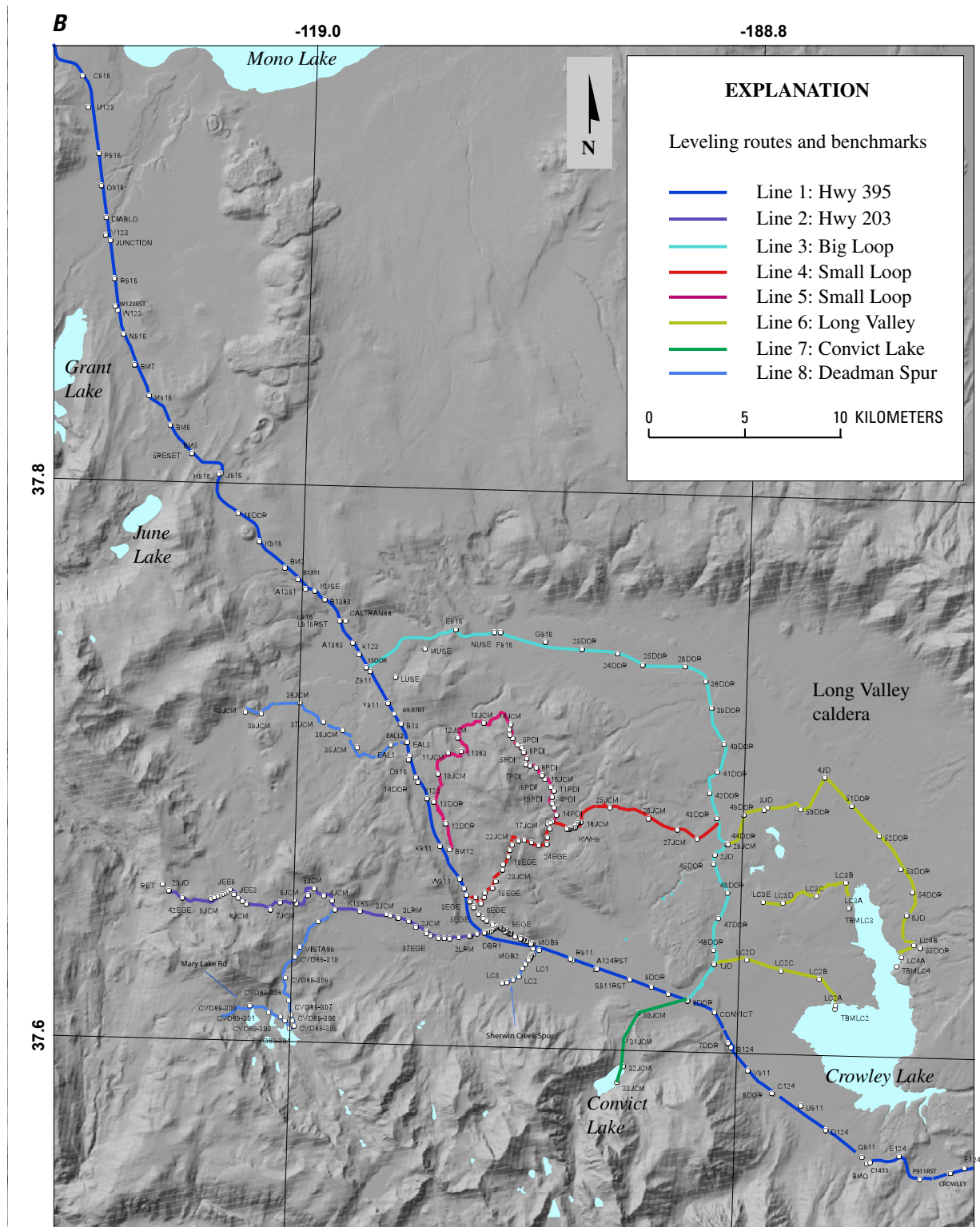


Figure 1. (A) Map of Long Valley volcanic region with GPS on leveled Bench Mark (GPSBM) sites and leveling routes. The GPSBM 03 label identifies the sites belonging to the NGS GEOID03 data base, whereas GPSBM 2006 the sites occupied by the U.S. Geological Survey in July 2006; (B) Map of Long Valley leveling routes and benchmarks—Continued.

assess the accuracy of GEOID03 in the region, (2) improve the estimate of the local adjustment to the geoid height model, and (3) compute a precise geoid height model (LVGEOID) for the Long Valley volcanic region.

Our results show that while LVGEOID and GEOID03 closely coincide in areas outside the caldera, the two models differ by as much as 0.2 m within the caldera. Accounting for this difference is critical when using a geoid height model to estimate ground deformation due to magmatic and tectonic unrest within the caldera.

Comparing GPS and Leveling

Before vertical GPS measurements can be compared with leveled heights to obtain vertical displacements, the heights must be transformed into the same reference frame (fig. 2). The reference surface for leveling is the geoid, an equipotential surface closely identified with mean sea level (Rapp, 1980). To obtain a homogeneous set of elevations from different leveling surveys, raw leveling heights must be referenced to a common vertical datum. The present vertical datum for the United States is the North American Vertical Datum of 1988 (NAVD88). NAVD88 elevations are expressed by Helmert orthometric heights, which can be computed using the Helmert orthometric reduction (Zilkoski and others, 1992). GPS solutions, however, produce a set of XYZ coordinates that are referenced to the center of an ellipsoid that approximates the Earth's surface. To obtain heights from GPS solutions, the XYZ coordinates must be transformed into geodetic latitude, longitude, and ellipsoidal heights. This transformation is usually performed using the World Geodetic System WGS84 ellipsoid model (Snay and Soler, 2000). In the conterminous United States, horizontal coordinates in WGS84 are practically identical to those of the present North American horizontal Datum of 1983 (NAD83); the two systems agree at the 0.1 mm level (Langley, 1992). Geoid and ellip-

soid surfaces, however, do not coincide. The vertical distance between the ellipsoid and the geoid is called the geoid height or the ellipsoid-geoid separation, N . An elevation measured with respect to the geoid (for example, by leveling) is called an orthometric height, and an elevation determined with respect to the reference ellipsoid (for example, by GPS) is called an ellipsoidal height. The value of N ranges from -100 m in Sri Lanka to +70 m in the Marianas Trench. GPS heights can be transformed into the same reference frame as leveled heights by using an appropriate geoid height model (Smith and Milbert, 1999). Geoid height models developed by the National Geodetic Survey enable one to directly convert between NAD83 GPS heights and NAVD88 leveling heights within the United States (<http://www.ngs.noaa.gov/GEOID/>).

Leveling

Beginning in 1975, a series of repeated leveling surveys, in which orthometric height differences between stations are measured with a precise optical level, have been used to measure vertical deformation along the 65-km-long line along Hwy 365 from Tom's Place to Lee Vining and along several other routes within Long Valley caldera (fig. 1B; tables 1–5 are at the back of this report). Bench mark C916 (fig. 1) is the elevation datum for all the leveling surveys. In other words, the height of C916 is assumed to be fixed. This assumption introduces a small bias in heights determined by any given survey, but it does not affect the shape of the vertical displacement field computed by differencing two surveys. The magnitude of the bias is unknown, but the flat shape of vertical displacement profiles along Hwy 395 in the vicinity of C916 suggests that any real motion there is small (that is, no more than a few millimeters).

The Highway 395 route was surveyed in 1932, 1957, 1975, 1980, each summer from 1982 to 1988, 1992, 1995, 1997 and 2006. Complete leveling of the caldera occurred each summer from 1982 to 1986, and in 1988 and 1992 (Langbein and others, 1995). The leveling surveys were run to standards equal to those required for first-order, class II surveys, as established by the National Geodetic Survey (Federal Geodetic Control Committee, 1984). The standard error for height differences between marks determined by a single survey can be taken to be $0.7 \text{ mm} \cdot \text{km}^{1/2}/L^{1/2}$, where L is the cumulative distance between bench marks in km (<http://www.ngs.noaa.gov/heightmod/Leveling/requirements.html>). The standard (white noise) error for height changes computed by differencing results of two surveys is $1.0 \text{ mm} \cdot \text{km}^{1/2}/L^{1/2}$. Leveling observations were corrected for rod scale and temperature, level collimation, and for astronomic, refraction and magnetic effects (Balazs and Young, 1982). In general, leveling surveys are not referenced to the NAVD88 datum because the U.S. Geological Survey (USGS) is mainly interested in monitoring relative elevation changes within the caldera, rather than determining absolute elevations.

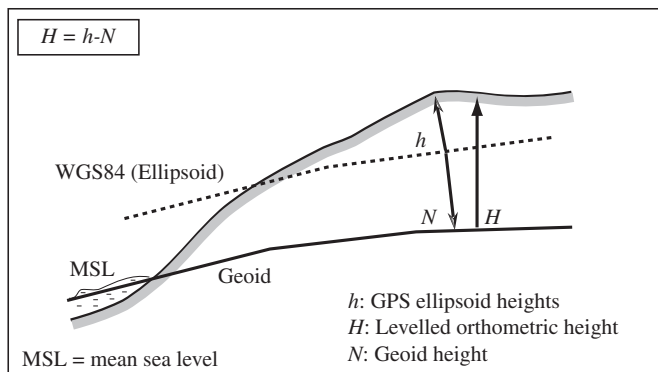


Figure 2. Relationship between the ellipsoid height h , orthometric height H , and geoid height N .

Helmert Orthometric Heights

The first stage in the computation of a geoid height model within Long Valley Caldera requires the 2006 leveling survey to be referenced to the NAVD88 vertical datum by transforming the raw leveling heights into Helmert orthometric heights (Milbert and Smith, 1996). The NAVD 88 datum is expressed in Helmert orthometric heights, and was computed in 1991. The NAVD 88 datum was realized by a single datum point, Father Point/Rimouski, in Quebec, Canada. The strategy and the value of the constraint were based on a number of factors. But, the foremost requirement was to minimize recompilation of national mapping products.

The transformation is a two-step process – (1) the geopotential number associated with a leveling bench mark is computed, and (2), the Helmert height using the orthometric reduction formula (Heiskanen and Moritz, 1967, p. 167) is calculated.

The geopotential number C_B represents the difference between the potential at the geoid and the potential at the observation point B on the Earth's surface (Heiskanen and Moritz, 1967, p. 162)

$$C_B = W_0 - W_B = \int_0^{h_B} g dh, \quad (1)$$

where 0 is a point at mean sea level (on the geoid), h_B is the raw leveling height at point B relative to 0, g is the external gravity (a function of the elevation h), and W is the gravitational potential. If A is the leveling survey datum (or primary base station) and B a second point on the leveling route, we have

$$C_B = W_0 - W_B = (W_0 - W_A) + (W_A - W_B) = C_A + \int_{h_A}^{h_B} g dh, \quad (2)$$

For normal orthometric heights, C_A is given by (Heiskanen and Moritz, 1967, p. 162)

$$C_A = \gamma_0 H^{dyn}, \quad (3)$$

where H^{dyn} is a local dynamic height expressed in the NAVD88 vertical datum and γ_0 is, by convention, the normal gravity value computed on the Geodetic Reference System ellipsoid of 1980 (GRS80) at 45° degrees latitude. Dynamic heights scale the geopotential number by a global constant $\gamma_0 = 980.6199$ gal, converting the geopotential number into a length. The dynamic height for the bench mark C916 (the elevation datum for the Long Valley Caldera leveling network) is $H^{dyn} = 2071.409$ m (see the data sheet for C916, PID = HR0097, available from the NGS server at <http://www.ngs.noaa.gov/cgi-bin/datasheet.pr1>). To solve the integral in equation , values of

the surface gravity g at every leveling bench mark between A and B are necessary. These values may be computed using the NAVD 88 Modeled Gravity software, available from the NGS server at <http://www.ngs.noaa.gov/TOOLS>. Geopotential numbers are measured in g.p.u. (geopotential units), where 1 g.p.u. = 1 kgal m = 1 ms-2 m.

To compute the orthometric height at B , C_B is substituted into the Helmert's height reduction formula (Heiskanen and Moritz, 1967, p. 167)

$$H_B = \frac{C_B}{\bar{g}} = \frac{C_B}{g + 0.0424 H_B}, \quad (4)$$

where HB is the orthometric height expressed in 10^3 m and \bar{g} is the mean value of the gravity along the plumb line between the geoid and the surface. Using the simplified Prey reduction formula for the gravity, then $\bar{g} = g + 0.0424 H_B$ (Heiskanen and Moritz, 1967, p. 167), where g is the gravitational acceleration at B expressed in gal (1 gal = 0.01 m/s²). The approximated formula (4) is often sufficient for standard topography. Solving the algebraic equation yields the value for the orthometric height at the leveling bench mark B

$$H_B = \frac{-g + \sqrt{g^2 + 4 \times 0.0424 C_B}}{2 \times 0.0424}, \quad (5)$$

Orthometric heights for the 2006 leveling survey are shown in table 1. The difference between the lowest (U123) and the highest (RET) leveled elevations is about 750 m. The standard errors for orthometric heights, taken to be the same as those of the leveled elevations (Zilkoski and others, 1992), range from 1 mm (station U123) to 6 mm (station F124) and average 5 mm within the caldera.

GPS Ellipsoidal Heights

During the GPS survey in 2006, phase and pseudorange data were recorded on Ashtech Z-12 and Z-Xtreme receivers using Dorne-Margolin choke-ring antennas. Data were recorded for sessions that lasted at least 6 hours at every sites. GPS survey sites were chosen based on their relatively uniform spacing along the leveling lines and good sky view (to maximize the data quality). At some locations, 5JCM and 18EG in particular, the sky view was not completely clear but was better than other nearby leveling sites.

GPS data were processed with the Gipsy/Oasis II software (Lichten and Border, 1987), using a bias-fixed, fiducial-free, precise point positioning strategy (Zumberge and others, 1997). We did not solve for the satellite orbits or clock errors, using instead solutions for these parameters provided by the Jet Propulsion Laboratory (JPL). Further precision was obtained by regional filtering, which removes most of com-

6 Converting NAD83 GPS Heights Into NAVD88 Elevations With LVGEOID, Long Valley Volcanic Region, California

mon-mode signals (Wdowinski and others, 1997). An elevation mask of 15 degrees was used during data processing.

We included a globally distributed subset of IGS stations, typically 25 to 30 stations, in our solutions. Using the ITRF00 positions of these stations, a Helmert transformation was done to transform each daily solution into the ITRF00 reference frame. The ITRF00 XYZ solutions were transformed into geodetic latitude, longitude, and ellipsoidal heights using the NAD83 ellipsoidal model for the conterminous United States and the Horizontal Time Dependent Positioning (HTDP) software, available from the NGS server at <http://www.ngs.noaa.gov/TOOLS>. GPS ellipsoid heights and their uncertainties for the 2006 survey are reported in table 2. The formal errors obtained in the GIPSY solutions have been scaled by a factor of two to produce a scaled formal error level that approximates the observed RMS about the linear fit to the time series. The errors also include both white noise and random walk components (Prescott and others, 2001). Uncertainties in the GPS ellipsoidal heights range from 12 mm (station D124) to 42 mm (station 5JCM), averaging 19 mm.

The Geoid Height Model

Equation (6) gives the general relationship between ellipsoid heights (heights between the external surface and the ellipsoid), h , orthometric heights (heights between the external surface and the geoid), H , and geoid height (distance between the ellipsoid and the geoid), N (see fig. 2)

$$h = H + N, \quad (6)$$

In the conterminous United States, the geoid surface is beneath the ellipsoid; thus, geoid heights N are negative, and the ellipsoidal height h is smaller in magnitude than the orthometric height H at a given point. By subtracting the orthometric heights H from the ellipsoid heights h , we obtain the geoid heights N (Milbert and Smith, 1996).

Gravity points, digital elevations, and altimetrically derived gravity anomalies can be processed to compute a geocentric gravimetric geoid height model (Smith, 1998; Roman and others, 2004). We cannot, however, transform directly between NAD83 GPS ellipsoid heights and NAVD88 orthometric heights using a gravimetric geoid. There is a systematic offset between the NAVD 88 reference level and the current best estimate of global mean sea level, and a transcontinental tilt is introduced by the non-geocentricity of the NAD83 ellipsoid (Smith and Milbert, 1999), which prevents the conversion. To complete the transformation between GPS ellipsoid heights and orthometric heights, the gravimetric geoid height N , the ellipsoidal heights h and the orthometric heights H must be related through an empirical conversion surface s (Milbert, 1995; Kotsakis and Sideris, 1999). If subscripts are used to denote the height reference systems, then we can rewrite as

$$H_{88} = h_{83} - (N+s), \quad (7)$$

where H_{88} indicates the GPS-based orthometric heights relative to NAVD88 and h_{83} the GPS ellipsoid heights relative to NAD83. The new geoid model $N+s$ is called a hybrid geoid (Smith and Milbert, 1999). The most recent gravimetric geoid model (USGG2003) and hybrid geoid model (GEOID03) for the conterminous United States were released by the National Geodetic Survey in December 2003 (Roman and others, 2004; <http://www.ngs.noaa.gov/GEOID/>). Using these models, the leveled orthometric heights H_{88} (table 1) can be subtracted from the GPS ellipsoid heights h_{83} (table 2) to compute the experimental value of the hybrid geoid model $N+s$ at the 25 colocated leveling and GPS benchmarks in Long Valley Caldera (table 3).

The measured geoid height model can then be compared against the published NGS GEOID03 model (fig. 3). The profiles shown in fig. 3 indicate that the geoid shapes are similar, but the NGS model underestimates the geoid height within the caldera. In particular, the difference reaches a maximum at sites on the caldera's resurgent dome and appears negligible at Lee Vining and Tom's Place, outside the caldera to the north and south, respectively. The GEOID03 model is globally accurate but requires a local adjustment (Smith and Roman, 1999), probably because the NGS used only six GPS/leveling comparisons (BRIDGEPORT, E 818, JUCTION, OASIS, T 1391, X 123) to estimate the conversion surface s in Mono County (<http://www.ngs.noaa.gov/GEOID/GPSonBM03/index.html>), and only two of these sites (JUCTION and X 123) are within the Long Valley volcanic region (fig. 1A). It is worth noting that the 4th site along Hwy 395 (T2SR, approximately at km 20) and the 2nd site along Hwy 203 (PM14, approximately at km 5) show a suspiciously large difference between the geoids and can probably be considered as outliers. These outliers may reflect local anomalies in the gravity field.

The Long Valley Caldera Hybrid Geoid Height Model LVGEOID

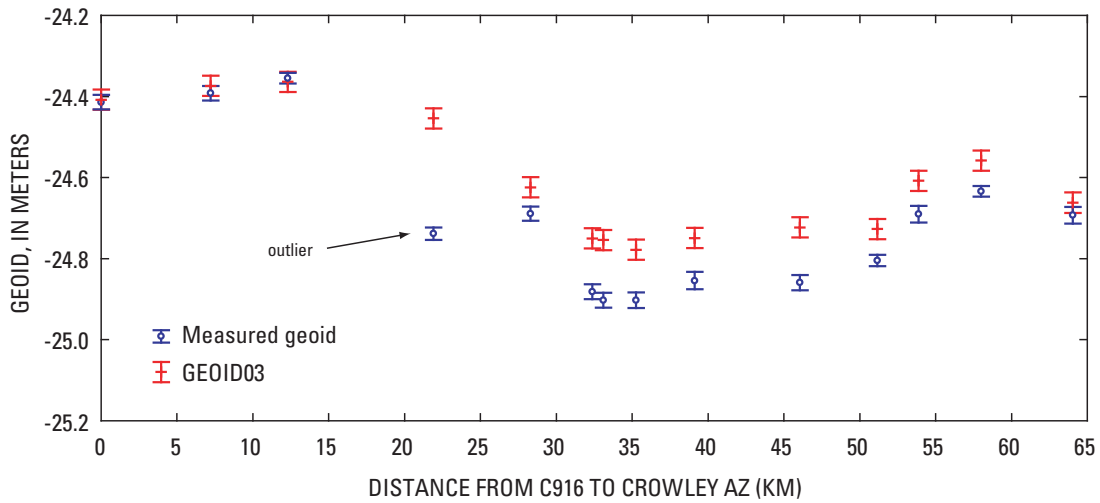
Conversion surface

Following Milbert and Smith (1996), we modeled a “locally adjusted” conversion surface s to improve the hybrid geoid for Long Valley Caldera. As a first step, we computed the conversion surface s at the colocated sites (table 4)

$$s = h_{83} - N_{03} - H_{88}, \quad (8)$$

where N_{03} is the gravimetric geoid USGG2003 height. Then we interpolated the “locally corrected” conversion surface s at sites where we have no direct measurements. Finally, we estimated the interpolation error (see appendix for details). We

A) Hwy 395



B) Hwy 203 - Long Valley

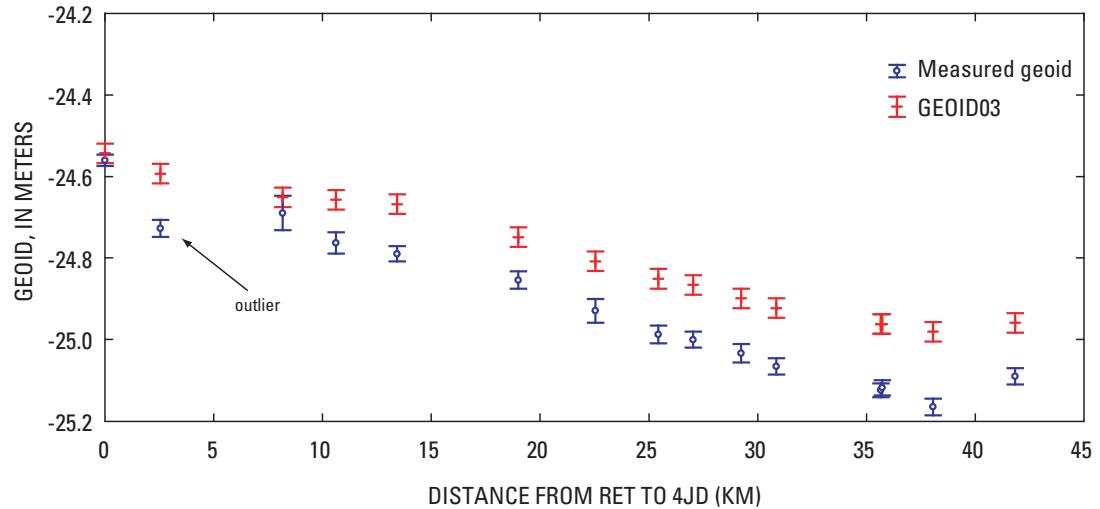


Figure 3. Profiles of the measured geoid and GEOID03 along the GPS-on-Bench Mark sites in the Long Valley region. Hwy 395 (A) crosses Long Valley caldera from north to south (the caldera extends approximately between the 30 km and 50 km distances along the leveling route), whereas Hwy 203 - Long Valley (B) crosses Long Valley caldera from west to east. See fig. 1 for bench mark locations. The 4th site along HWY 395 (T2SR, approximately at km 20) and the 2nd site along Hwy 203 (PM14, approximately at km 5) show a suspiciously large difference between the geoids and can probably be considered as outliers.

8 Converting NAD83 GPS Heights Into NAVD88 Elevations With LVGEOID, Long Valley Volcanic Region, California

calculated the new “locally adjusted” hybrid geoid height at each leveling bench mark (see table 5) by adding s to the NGS gravimetric geoid USGG2003 (Smith and Roman, 1999). The stated uncertainties in the “locally corrected” hybrid geoid model are from the propagation of errors from interpolation only, since there is no formal accuracy estimate for the gravimetric geoid (Roman, NGS, written commun.). Geoid uncertainties average 0.022 m with a median value of 0.021 m and a standard deviation of 0.008 m.

A plot of the “locally corrected” geoid LVGEOID against GEOID03 is shown in fig. 4, whereas the spatial distribution of the difference between LVGEOID and GEOID03 is shown in fig. 5.

Summary and Conclusions

We have tied GPS and leveling to a common reference frame in the Long Valley area so that we can compute the vertical deformation by differencing GPS-based and leveled orthometric heights. To transform directly between GPS ellipsoid heights and orthometric heights, we related the gravimetric geoid height N , the ellipsoidal heights h , and the orthometric heights H through an empirical conversion surface s . The new geoid model $N+s$ is called a hybrid geoid (Smith and Milbert, 1999). In December 2003, the National Geodetic Survey released the latest gravimetric geoid model (USGG2003) and hybrid geoid model (GEOID03) for the conterminous United States.

We compared the NGS GEOID03 model against the experimental values of the geoid height measured at 25 GPSBM sites. These sites were occupied in the summer of 2006 by both GPS and leveling surveys. From the profiles shown in figure 3, we can see that although the geoid shapes are similar, the NGS model underestimates the geoid height within the caldera. The difference reaches a maximum of 18.5 cm close to the caldera’s resurgent dome and appears negligible at Lee Vining and Tom’s Place, outside the caldera.

We used geostatistics (ordinary kriging and Gaussian simulation) to estimate the new conversion surface s in the

Long Valley region at any unsampled leveling benchmark from the 25 available data points. We calculated the new “locally adjusted” hybrid geoid height (LVGEOID) at each leveling bench mark (see table 5) by adding s to the NGS gravimetric geoid USGG2003 (Smith and Roman, 1999). The average LVGEOID uncertainty of 0.022 m compares well with the published uncertainty for GEOID03 (0.024 m).

A quantitative check can be made by comparing the vertical displacements calculated for the intervals 1985 to 1999 and 1985 to 2006 using the different geoid height models (fig. 6). There are several reasons to choose these intervals – (1) Electronic Distance Measurement (EDM) coverage of the caldera began in 1985; (2) in 1999, Battaglia and others (2003) performed GPS surveys on Bench Marks in the Long Valley volcanic region; (3) the latest leveling survey was in 2006; and (4) continuous GPS results suggest that as little as 4 to 7 mm of net vertical displacement occurred from 1999 to 2006 (fig. 7; <http://quake.wr.usgs.gov/research/deformation/gps/auto/LongValley/rdom/index.html>). Although the 1999–1985 GPS-leveling vertical deformation estimated using LVGEOID compares satisfactorily with the 2006–1985 leveling-leveling uplift, both GEOID03 and GEOID99 underestimate the GPS based orthometric heights for 1999, and thus the vertical deformation between 1999 and 1985. At the resurgent dome (the area with the most pronounced deformation in Long Valley Caldera), the deformation determined used the NGS geoid is underestimated by 0.10 to 0.15 m.

The geodetic data set for the 1999–85 differences (44 height measurements, and 34 EDM baseline length changes) can be inverted to have an estimate of the parameters of the intrusion beneath the resurgent dome. A prolate spheroidal source is used to parameterize the horizontal and vertical deformation. The inversion of the data is performed using a weighted least square algorithm, whereas the penalty function minima are searched by a Nelder-Mead simplex direct search algorithm. A bootstrap algorithm is used to estimate the 95 percent (two standard deviations) bounds on the parameters. Preliminary results (see table 6) point to a deeper, larger source than that previously inferred.

Table 6. Ninty-five-percent (two standard deviations) bounds on intrusion source parameters.

	GEOID99 (after Battaglia and others, 2003)	LVGEOID
X (UTM)	332188	332411
Y (UTM)	4172064	4171963
Depth (km)	4.9	7.6
Aspect ratio	0.25	0.65
Volume change (km^3)	0.06	0.13

[§] Dimensionless pressure: pressure change/shear modulus.

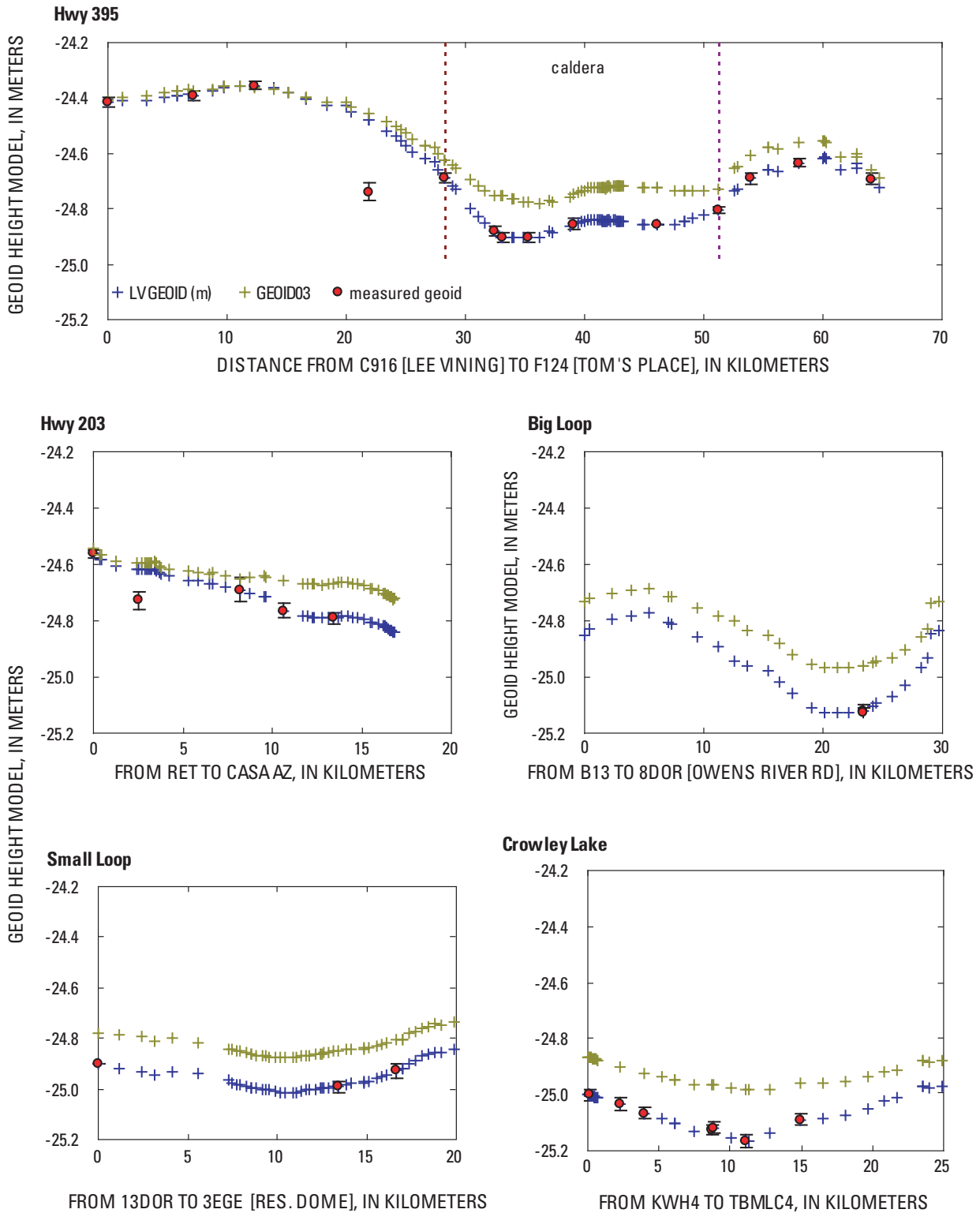


Figure 4. Geoid height profiles from leveling surveys in the Long Valley region. The two outliers are benchmarks T2SR (Hwy 395) and PM14 (Hwy 203).

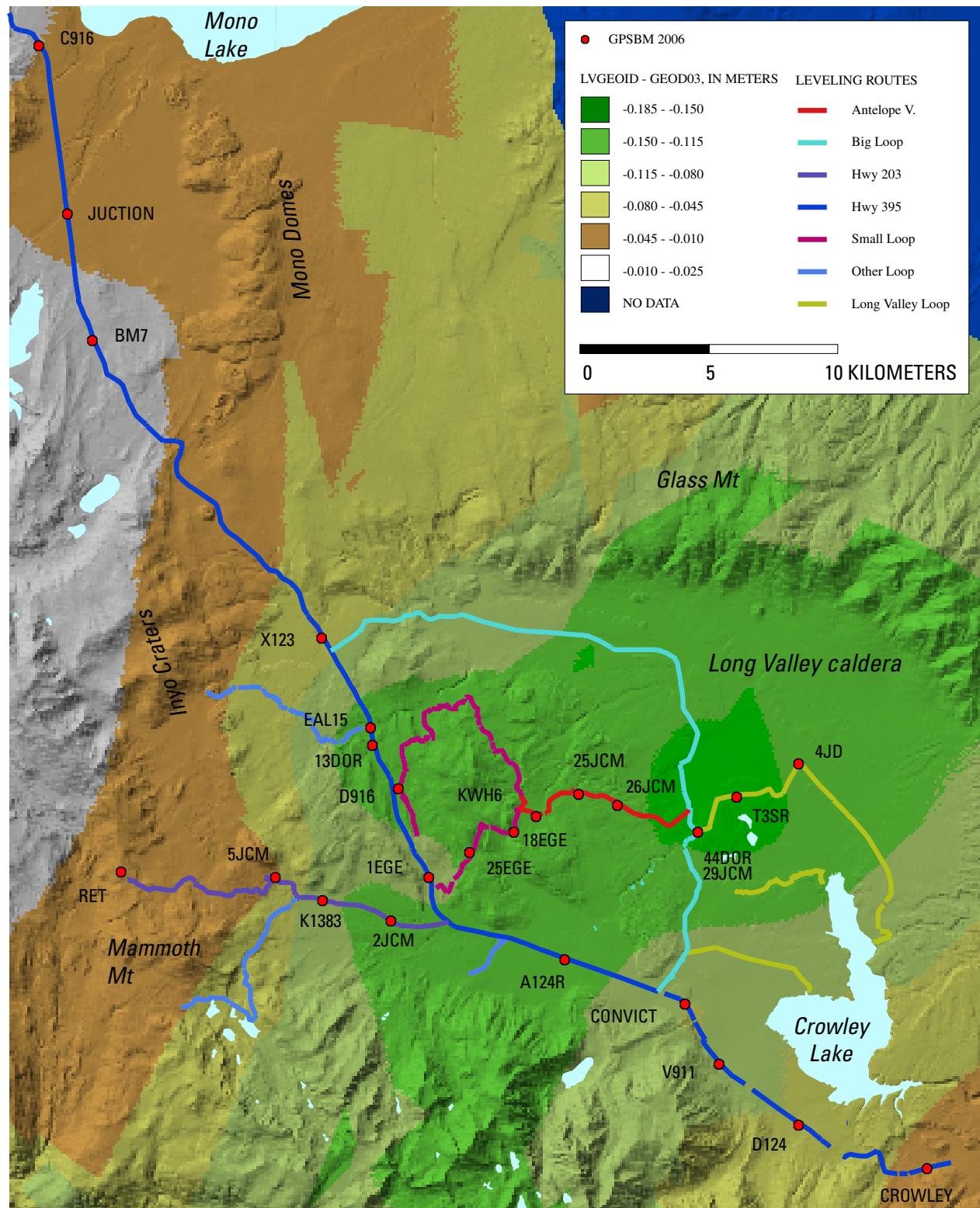


Figure 5. Map of the difference between LVGEOD and the GEOID03 NGS geoid height model in the Long Valley region.

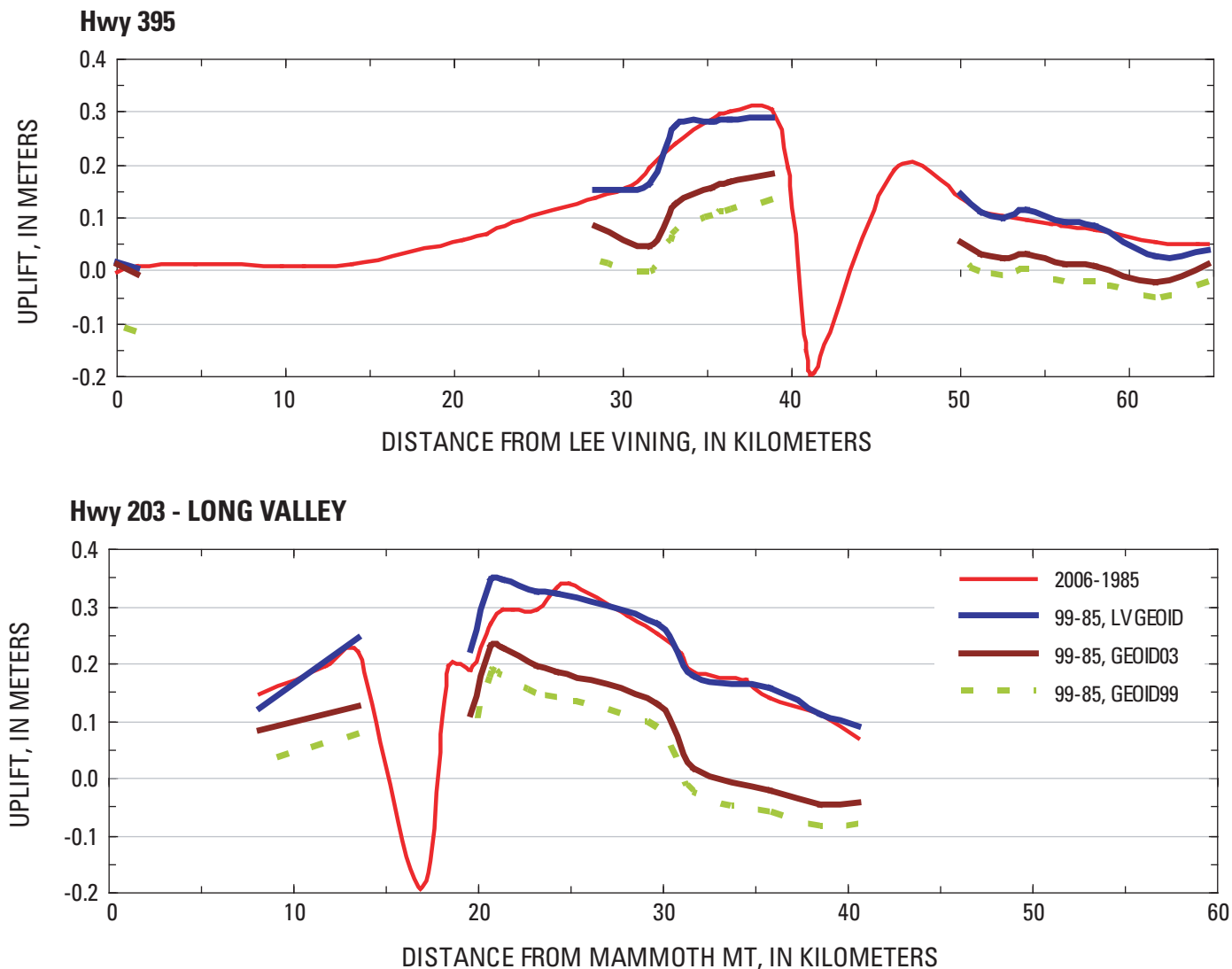


Figure 6. Vertical deformation in the Long Valley region measured along the two leveling routes occupied in the summer of 2006. 2006-1985 is the deformation computed by differencing the 2006 and 1985 leveling surveys. The other three lines show the deformation between 1999 and 1985 obtained differencing the 1999 GPS based orthometric heights and the 1985 leveled orthometric heights. LVGEOD, GEOID03, and GEOID99 are the three geoid height models employed to compute the GPS based orthometric heights.

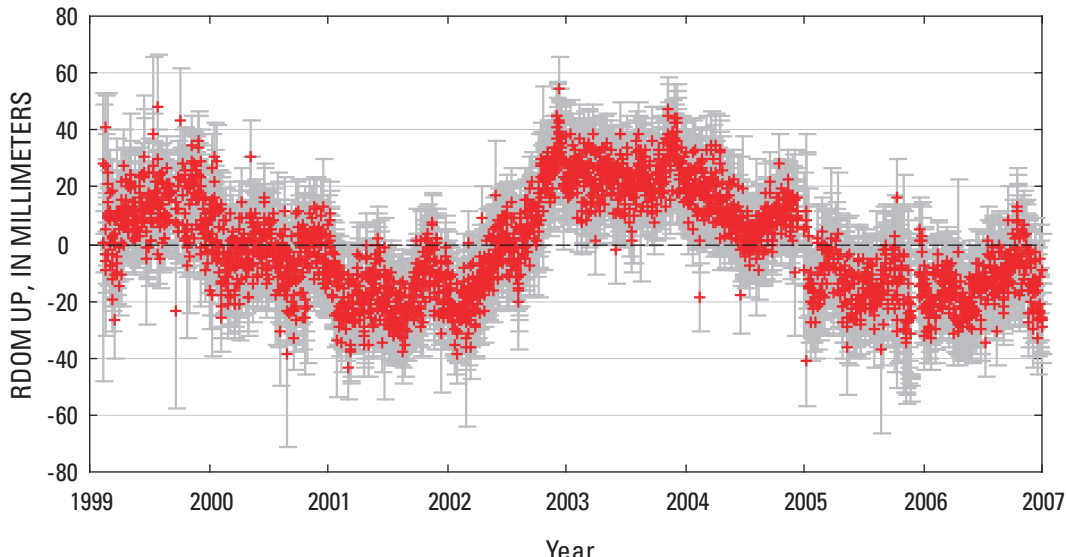


Figure 7. Vertical deformation at the permanent GPS site RDOM in Long Valley Caldera. The site is on the caldera resurgent dome (see also fig. 1A). Vertical velocity is 0.6 to 1.0 mm/yr. In the 7 years between the 1999 GPS ellipsoid heights on leveled on bench marks (GPS-on-Bench Mark) and the 2006 GPS and leveling surveys, the expected deformation is on the order of 4 to 7 mm (<http://quake.wr.usgs.gov/research/deformation/gps/auto/LongValley/rdom/index.html>).

Acknowledgments

Comments from J. Murray and M. Poland greatly helped to improve the manuscript.

References Cited

- Balazs, E.I., Young, G.M., 1982, Corrections applied by the National Geodetic Survey to precise leveling observations: National Oceanic and Atmospheric Administration Technical Memorandum, NOS-NGS 34, 12 p.
- Battaglia, M., Segall, P., Murray, J., Cervelli, P. and Langbein, J. 2003, The mechanics of unrest at Long Valley caldera, California; 1-Modeling the geometry of the source using GPS, leveling and 2-color EDM data: Journal of Volcanology and Geothermal Research, v. 127, p. 195-217
- Goovaerts, P., 1997, Geostatistics for Natural resources Evaluation: Oxford University Press, New York, N.Y.
- Heiskanen, W., and Moritz, H., 1967, Physical Geodesy. W.H. Freeman, San Francisco, Calif.
- Kotsakis, C., and Sideris, M.G., 1999, On the adjustment of combined GPS/levelling/geoid networks: *Journal of Geodesy*, v. 73, p. 412-421.
- Langbein, J., Dzurisin, D., Marshall, G., Stein, R., and Rundle, J., 1995, Shallow and peripheral volcanic sources of inflation revealed by modeling two-color geodimeter and leveling data from Long Valley Caldera, California, 1988-1992: *Journal of Geophysical Research*, v. 100, p. 12487-12495.
- Langley, R.B., 1992, Basic geodesy for GPS: *GPS World*, v. 92, p. 44-49.
- Lichten, S.M., and Border, J.S., 1987, Strategies for high-precision global positioning system orbit determination: *Journal of Geophysical Research*, v. 92, p. 12751-12762.
- Milbert, D.G., 1998, Documentation for the GPS Benchmark Data Set of 23-July-98, Bulletin N. 8, International Geoid Service, Milan, p. 29-42.
- Milbert, D.G., 1995, Improvement of a high resolution geoid height model in the United States by GPS height on NAVD88 bench marks-New geoids in the world: *Bulletin d'Information, Bureau Gravimetrique International* 0373-9023, v. 77, p. 13-36.

Milbert, D.G., and Smith, D.A., 1996, Converting GPS Height into NAVD 88 Elevation with the GEOID96 Geoid Height Model; GIS/LIS '96 Annual Conference and Exposition: American Congress on Surveying and Mapping, Washington, D.C., p. 681-692.

Prescott, W.H., J.C. Savage, J.L. Svare, and Manaker, D., 2001, Deformation across the Pacific-North America plate boundary near San Francisco, California: Journal of Geophysical Research, v. 106, B4, p. 6673-6682, 10.1029/2000JB900397.

Rapp, R.H., 1980, Precise definition of the geoid and its realization for vertical datum applications: Proceedings 2nd International Symposium on Problems Related to the Redefinition of North American Vertical Geodetic Networks, the Canadian Institute of Surveying, Ottawa, p. 73-86.

Roman, D.R., Wang, Y.M., Henning, W., and Hamilton, J., 2004, Assessment of the New National Geoid Height Model, GEOID03: Proceedings of the 2004 ACSM/TAPS Conference and Technology Exhibition, Nashville, Tenn., April 16-21, 2004.

Smith, D.A., 1998, There is no such thing as "The" EGM96 geoid-Subtle points on the use of a global geopotential model: Bulletin no. 8, International Geoid Service, Milan, 1998, p. 17-28.

Smith, D., and Milbert, D.G., 1999, The GEOID96 high-resolution geoid height model for the United States: Journal of Geodesy, v. 73, p. 219-236.

Snay, A., and Soler, T., 2000, Modern Terrestrial reference Systems, part 3: WGS84 and ITRS. Professional Survey, v. 3, p. 1-3.

Wdowinski, S., Bock, Y., Zhang, J., Fang, P., and Genrich J., 1997, Southern California Permanent GPS Geodetic Array: Spatial Filtering of Daily Positions Estimating Coseismic and Postseismic Displacements Induced by the 1992 Landers Earthquake: Journal of Geophysical Research, v. 102, p. 18057-18070.

Zilkoski, D.B., Richards, J.H., and Young, G.M., 1992, Results of the general adjustment of the North American Vertical datum of 1988: Surveying and Land Information Systems, v. 52, p. 133-149.

Zumberge, J.F., Heflin, M.B., Jefferson, D.C., Watkins, M.M., and Webb, F.H., 1997, Precise point positioning for the efficient and robust analysis of GPS data from large networks: Journal of Geophysical Research, v. 102, p. 5005-5017.

Appendix. Geostatistical Analysis

Spatial Interpolation

We used ordinary kriging, a linear least-square regression algorithm, to estimate the experimental conversion surface s at unsampled leveling benchmarks (Goovaerts, 1997, p. 132). The geostatistical analysis and interpolation was carried out using the geostatistical software library GSLIB (Deutsch and Journel, 1998; <http://www.gslib.com/>). Kriging interpolates the value of the continuous attribute s at any unsampled locations u using only the values of s available over our study area, the data $s(\mathbf{u}_\alpha)$ (see figure 8 and table 4).

The linear estimator is defined as

$$s(\mathbf{u}) - m(\mathbf{u}) = \sum_{\alpha=1}^{n(\mathbf{u})} \lambda_\alpha(\mathbf{u}) [s(\mathbf{u}_\alpha) - m(\mathbf{u}_\alpha)], \quad (9)$$

where $\lambda_\alpha(\mathbf{u})$ is the weight assigned to the datum $s(\mathbf{u}_\alpha)$, and the quantities $m(\mathbf{u})$ and $m(\mathbf{u}_\alpha)$ are the expected values (means) of $s(\mathbf{u})$ and $s(\mathbf{u}_\alpha)$. The number of data involved in the estimation, as well as their weights, may change from one location to another. In practice, only the $n(\mathbf{u})$ data within a

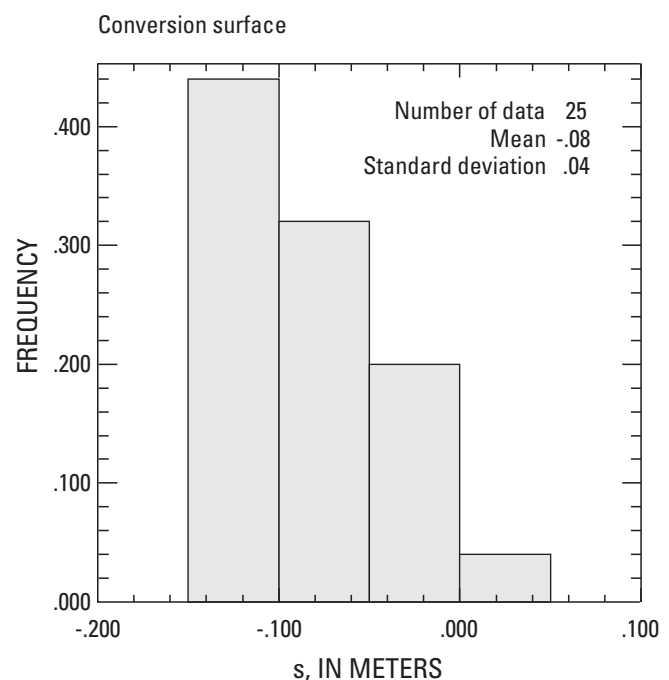


Figure 8. Histogram of the conversion surface. Compare this non-Gaussian distribution with the normal distribution in figure 10 obtained through the transformation described in the accompanying text.

given neighborhood $W(\mathbf{u})$, centered on the location \mathbf{u} being estimated, are retained. Ordinary kriging accounts for local fluctuations of the mean assuming that $m(\mathbf{u})$ is constant, but unknown, within $W(\mathbf{u})$ (Goovaerts, 1997, p. 126). It is well known that kriging smoothes the fit of a curve or surface to data and that the histogram of the values estimated by kriging will display more values around the mean but less extreme values than the histogram of the observations (for example, Biau and others, 1999).

The key function in the interpolation is the variogram $\lambda_\alpha(\mathbf{u})$. The variogram describes the spatial dependence of s , and is used to calculate the weights $\lambda_\alpha(\mathbf{u})$ and the mean $m(\mathbf{u})$ applied in . Typically, the variogram function is inferred and modeled from the experimental variogram computed from the experimental data (Goovaerts, 1997, p. 82; fig. 9). Variogram models can be divided into two types; those that reach a plateau (called a “sill”, and designated as c) and those that do not. The distance at which they reach this plateau is called the “range,” a . The variogram discontinuity at the origin is called the “nugget effect,” n . More than one theoretical model can fit the experimental variogram (fig. 9).

We choose the best model using cross-validation (Isaaks and Srivastava, 1989, ch. 15). In cross-validation, actual data points are dropped one at a time and re-estimated using

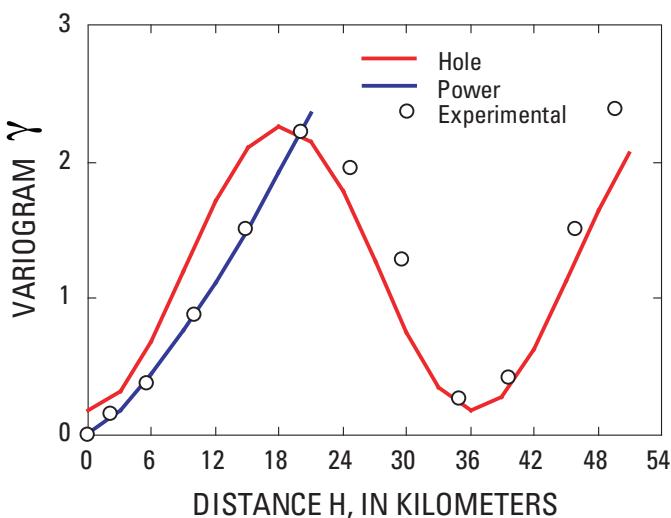


Figure 9. The conversion surface variogram inferred from the 25 measured values. Hole effect model defined by a length a to the first peak and positive variance contribution c . Power model defined by a power $0 < \omega < 2$ and positive slope c . n is the nugget effect (Deutsch and Journel, 1998, p. 28).

- Hole (a, c, n : 18.2112 1.0403 0.1794) - $\gamma_H(h) = c \cdot [1 - \cos(\pi h/a)]$
- Power (ω, c, n : 0.0399 1.3382 0.0122) - $\gamma_P(h) = c \cdot h^\omega$

the remaining neighboring data. Each datum is replaced in the data set once it has been re-estimated. We accepted the model with the highest correlation between true and estimated values (the power model for the conversion surface, see table 7). Although cross-validation can detect possible problems, it does not ensure that the interpolation will give “realistic” results (Journel, 1989). We report the interpolated values in table 5.

Table 7. Cross-validation of the variogram model for the conversion surface.

	Data	Power model	Hole model
Mean	-0.0845	-0.0893	-0.0868
Standard deviation	0.0449	0.0419	0.0409
Correlation		0.8269	0.7221

Assessment of Spatial Uncertainty

A by-product of kriging is the kriging variance, which is dependent on the variogram model and the data configuration, and is independent of the data values. Thus, given a variogram model, two identical data configurations would yield the same kriging variance no matter what the data were. In this sense, the kriging variance is only a ranking index of the data geometry and size (that is, the kriging variance increases when the location \mathbf{u} being estimated gets farther away from the data location \mathbf{u}_a)—not a measure of the local spread of errors (Goovaerts 1997, p. 179).

The smoothing effect of kriging on the interpolation is due to a missing error component. Consider the variable $S(\mathbf{u})$ as the sum of the estimator $s(\mathbf{u})$ and the corresponding error $r(\mathbf{u})$

$$S(\mathbf{u}) = s(\mathbf{u}) + r(\mathbf{u})$$

The kriging equation would provide the smoothly varying estimator $s(\mathbf{u})$. To restore the full variance of our geostatistical model, one may think of simulating a realization of the error with zero mean and the correct variance and variogram (Deutsch and Journel, 1998, p. 127). The simulated value of the variable would be the sum of the unique estimate and a simulated error value

$$s^{(s)}(\mathbf{u}) = s(\mathbf{u}) + r^{(s)}(\mathbf{u})$$

We applied a sequential Gaussian simulation algorithm to simulate the variable of interest s (Deutsch and Journel, 1998, p. 127). The standard deviation of the simulated variable is taken as measure of the interpolation error (Battaglia and others, 2003).

The Gaussian simulation works with data that follow a normal distribution. Even though most Earth science data do not follow a normal distribution, a nonlinear transformation can convert the original data distribution (fig. 8) into a normal distribution (fig. 10). The transformed data set is also called “normal score.” The simulation is performed in the normal space and repeated 500 times, and all the simulated values are back-transformed (Deutsch and Journel, 1998, p. 141). At any sampled point, the simulation algorithm returns the exact experimental value.

Just as in kriging, the variogram model is the key to any Gaussian simulation. Two models (hole and gaussian) fit the experimental normal score variogram (fig. 11). Although cross-validation (table 8) indicates that two models have practically identical performances, a statistical analysis of the simulation shows that the gaussian model better reproduces the overall statistics of the experimental data (fig. 10).

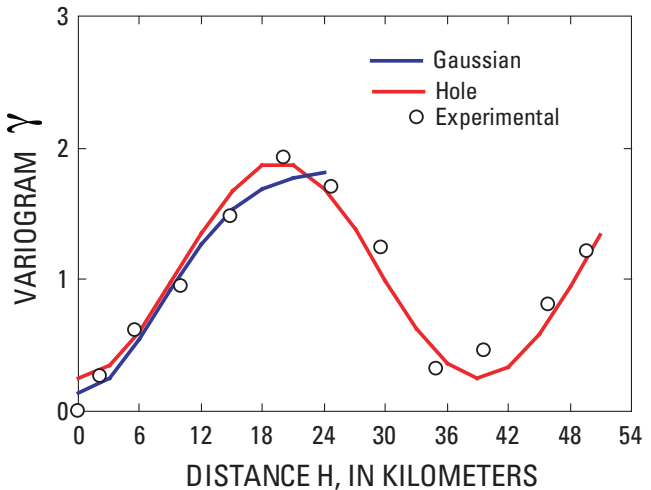


Figure 11. The normal score variogram inferred from the 25 measured values. Hole effect model defined by a length a to the first peak and positive variance contribution c ; Gaussian model defined by an effective range a and a positive variance contribution c ; and n is the nugget effect (Deutsch and Journel, 1998, p. 28).

Table 8. Cross-validation of the variogram model the normal score.

	Data	Gaussian model	Hole model
Mean	-0.0000	-0.0466	-0.0394
Standard deviation	0.09951	0.8715	0.8913
Correlation		0.5922	0.6011

- Hole (a, c, n : 19.5746 0.8188 0.2543 -
 $\gamma_H(h) = c \cdot [1 - \cos(\pi h/a)]$)
- Gaussian (a, c, n : 34.3768 1.6947 0.1340) -
 $\gamma_P(h) = c \cdot [1 - \exp(-9h^2/a^2)]$)
- Note that Gaussian model fit the data only for a limited distance. This is not a problem, because the best variogram model is chosen by cross-validation (see fig. 10).

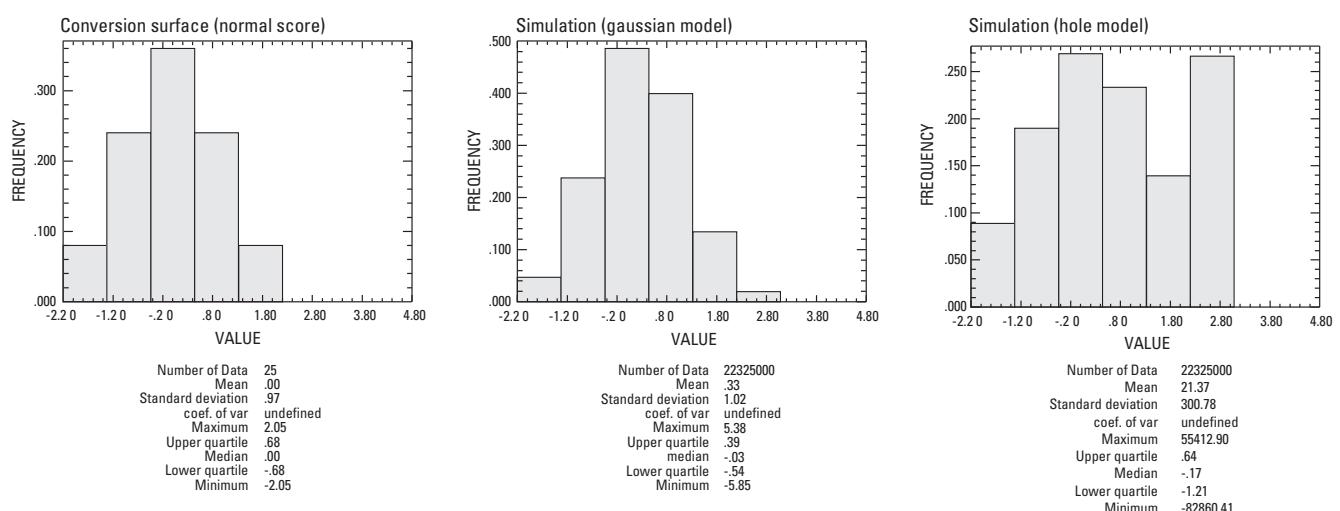


Figure 10. Histograms of the conversion surface (normal score) and the simulations. The gaussian model best reproduces the overall statistics of the normal score data set. The number of simulation data corresponds to 500 realizations of the conversion surface (normal score) on a grid of 190x235 cells, covering the Long Valley region from Lee Vining to Tom's Place. Each cell is 0.2x0.2 km in size.

Tables 1–5

Table 1. Leveling heights for the Long Valley region (see fig. 1B for bench mark locations).

BM ID	Distance	NAD 27				NAD 83		2006 leveling heights (m)		
		LAT (°)	W LONG (°)	X (UTM)	Y (UTM)	LAT (°)	LONG (°)	raw	ortho	σ
Hw 395										
C916	0	37.945556	119.103889	315132	4201661	37.94553	-119.10488	2072.542	2073.909	0.000
U123	1.18	37.934444	119.101111	315350	4200413	37.93433	-119.10208	2066.386	2067.759	0.001
Q916	4.67	37.906389	119.094444	315869	4197293	37.90633	-119.09538	2081.839	2083.219	0.002
DIABLO	5.87	37.895000	119.091944	316060	4196023	37.89493	-119.09288	2093.084	2094.467	0.002
V123	6.71	37.888611	119.091944	316045	4195313	37.88853	-119.09288	2091.156	2092.542	0.002
JUCTION	7.22	37.886667	119.089722	316233	4195097	37.88663	-119.09068	2101.939	2103.324	0.002
W123 RESET	9.72	37.863333	119.086944	316421	4192495	37.86323	-119.08788	2155.200	2156.603	0.002
N916	11.07	37.853333	119.082778	316757	4191378	37.85323	-119.08378	2190.014	2191.423	0.002
BM7	12.29	37.842500	119.077500	317197	4190169	37.84243	-119.07848	2220.981	2222.401	0.002
M916	13.87	37.831389	119.070833	317759	4188924	37.83133	-119.07178	2273.714	2275.144	0.003
5 RESET	16.66	37.811111	119.050833	319470	4186632	37.81103	-119.05178	2351.603	2353.077	0.003
J916	20	37.804167	119.037500	320624	4185841	37.80413	-119.03848	2403.222	2404.711	0.003
16DOR	20.44	37.790000	119.029444	321303	4184250	37.78993	-119.03038	2421.198	2422.707	0.003
K916	21.9	37.780000	119.019444	322160	4183121	37.77993	-119.02038	2437.253	2438.777	0.003
T2SR	21.91			322099	4183201	37.78064	-119.02109	2436.417	2438.180	0.003
BM2	23.43	37.770833	119.007778	323160	4182078	37.77073	-119.00878	2450.858	2452.376	0.003
B1391	24.18	37.766667	119.001667	323687	4181612	37.76663	-119.00268	2420.170	2421.685	0.003
A1391	24.64	37.763333	118.998056	323996	4181228	37.76323	-118.99908	2394.960	2396.478	0.003
B1383	25.6	37.759722	118.989444	324754	4180812	37.75963	-118.99038	2354.398	2355.902	0.004
CAL TRAN88	27.43	37.752222	118.979722	325591	4179962	37.75213	-118.98068	2285.610	2287.095	0.004
A1383	27.76	37.744444	118.976389	325864	4179090	37.74433	-118.97738	2280.117	2281.611	0.004
X123	28.29	37.740278	118.973333	326127	4178629	37.74023	-118.97427	2280.484	2281.984	0.004
Z911	29.17	37.734444	118.968333	326554	4177965	37.73433	-118.96927	2292.204	2293.712	0.004
Y911	30.45	37.723056	118.960000	327259	4176696	37.72303	-118.96097	2343.482	2345.025	0.004
B13	31.57	37.715833	118.953889	327780	4175875	37.71573	-118.95487	2332.277	2333.842	0.004
EAL15	32.37	37.709167	118.950833	328038	4175137	37.70913	-118.95177	2306.170	2307.738	0.004
EAL33	32.99	37.704444	118.949722	328124	4174602	37.70433	-118.95067	2320.826	2322.397	0.004
D916	33.09	37.703056	118.950000	328095	4174459	37.70303	-118.95097	2312.192	2313.766	0.004
Z1382 RESET	33.96	37.696667	118.946667	328371	4173742	37.69663	-118.94767	2323.264	2324.842	0.004
Y123	34.91	37.689167	118.941389	328821	4172901	37.68913	-118.94237	2315.532	2317.110	0.004
13DOR	35.25	37.688056	118.938333	329092	4172773	37.68803	-118.93927	2310.754	2312.335	0.004
12DOR	36.27	37.680278	118.932778	329559	4171897	37.68023	-118.93377	2311.056	2312.641	0.004
BM12	37.33	37.671111	118.930833	329714	4170873	37.67103	-118.93177	2309.546	2311.116	0.004
W911	38.81	37.660556	118.925833	330131	4169699	37.66053	-118.92677	2242.584	2244.130	0.004
1EGE	39.12	37.657222	118.923889	330291	4169318	37.65713	-118.92487	2233.810	2235.359	0.004

Table 1. Leveling heights for the Long Valley region (see fig. 1B for bench mark locations)—Continued.

BM ID	Distance	NAD 27				NAD 83		2006 leveling heights (m)		
		LAT (°)	W LONG (°)	X (UTM)	Y (UTM)	LAT (°)	LONG (°)	raw	ortho	σ
2EGE	39.42	37.655000	118.922778	330383	4169072	37.65493	-118.92377	2230.182	2231.734	0.004
3EGE	39.73	37.652500	118.921111	330527	4168791	37.65243	-118.92207	2230.089	2231.641	0.004
4EGE	40.03	37.650556	118.919444	330673	4168578	37.65053	-118.92037	2232.357	2233.906	0.004
5EGE	40.33	37.648056	118.917222	330862	4168296	37.64803	-118.91817	2238.275	2239.818	0.004
6EGE	40.6	37.646667	118.915000	331052	4168137	37.64663	-118.91597	2235.115	2236.654	0.004
Z123	40.79	37.645833	118.913333	331200	4168034	37.64573	-118.91427	2221.979	2223.518	0.004
7EGE	41.04	37.644722	118.910833	331419	4167907	37.64463	-118.91177	2216.631	2218.169	0.004
CASA AZ	41.27	37.643611	118.908056	331654	4167780	37.64353	-118.90907	2209.634	2211.173	0.004
DBR11	41.35	37.643889	118.908333	331637	4167814	37.64383	-118.90927	2209.989	2211.529	0.005
DBR8	41.53	37.643056	118.906111	331830	4167721	37.64303	-118.90707	2208.597	2210.136	0.005
DBR7	41.59	37.642778	118.905556	331873	4167687	37.64273	-118.90657	2208.757	2210.296	0.005
DBR6	41.65	37.642222	118.905000	331925	4167620	37.64213	-118.90597	2207.724	2209.263	0.005
DBR5	41.82	37.642222	118.904444	331978	4167619	37.64213	-118.90537	2207.446	2208.985	0.005
DBR2	42	37.641389	118.902778	332117	4167527	37.64133	-118.90377	2201.828	2203.370	0.005
DBR1	42.05	37.641111	118.902500	332143	4167493	37.64103	-118.90347	2198.549	2200.092	0.005
9EGE	42.14	37.641944	118.902500	332145	4167582	37.64183	-118.90347	2205.811	2207.354	0.005
MGB20	42.68	37.639722	118.897500	332581	4167329	37.63963	-118.89847	2193.343	2194.898	0.005
MGB19	42.73	37.639444	118.896667	332651	4167294	37.63933	-118.89767	2193.317	2194.870	0.005
MGB18	42.78	37.639444	118.896389	332677	4167294	37.63933	-118.89737	2192.796	2194.349	0.005
11EGE	42.83	37.639167	118.895833	332730	4167270	37.63913	-118.89677	2192.376	2193.926	0.005
MGB13	43.12	37.637778	118.893056	332965	4167110	37.63773	-118.89407	2190.744	2192.276	0.005
10DOR	44.96	37.632778	118.875278	334524	4166524	37.63273	-118.87626	2174.661	2176.196	0.005
A124 RESET	46.04	37.629444	118.863333	335576	4166125	37.62933	-118.86426	2168.642	2170.171	0.005
S911 RESET	47.53	37.625833	118.848333	336892	4165700	37.62573	-118.84926	2174.444	2175.963	0.005
9DOR RESET	48.38	37.623333	118.838611	337742	4165406	37.62323	-118.83956	2165.434	2166.948	0.005
T911 RESET	49.11	37.620833	118.830833	338425	4165115	37.62073	-118.83176	2158.041	2159.550	0.005
8DOR	50	37.618611	118.822222	339180	4164856	37.61853	-118.82316	2145.381	2146.883	0.005
CONVICT	51.16	37.614722	118.810000	340248	4164402	37.61463	-118.81096	2150.912	2152.398	0.005
7DOR	52.54	37.603611	118.803611	340789	4163160	37.60353	-118.80456	2099.466	2100.944	0.005
V911	53.87	37.593889	118.794444	341581	4162068	37.59383	-118.79536	2087.225	2088.710	0.005
6DOR	55.35	37.586111	118.783333	342545	4161184	37.58603	-118.78426	2108.880	2110.367	0.005
U911	56.23	37.581667	118.770278	343683	4160674	37.58163	-118.77126	2108.727	2110.208	0.005
D124	57.99	37.573056	118.758889	344672	4159701	37.57303	-118.75986	2112.663	2114.139	0.005
C1433	60.29	37.561944	118.738611	346442	4158425	37.56183	-118.73956	2142.561	2144.043	0.005
E124	61.49	37.564167	118.725556	347595	4158659	37.56413	-118.72656	2196.710	2198.206	0.005
P911 RESET	62.79	37.556111	118.716111	348418	4157745	37.55603	-118.71706	2149.444	2150.944	0.006

Table 1. Leveling heights for the Long Valley region (see fig. 1B for bench mark locations)—Continued.

BM ID	Distance	NAD 27			NAD 83		2006 leveling heights (m)			
		LAT (°)	W LONG (°)	X (UTM)	Y (UTM)	LAT (°)	LONG (°)	raw	ortho	σ
CROWLEY AZ	64.05	37.558611	118.702222	349651	4158000	37.55853	-118.70316	2133.982	2135.442	0.006
F124	64.67	37.560278	118.696111	350193	4158179	37.56023	-118.69706	2134.573	2136.026	0.006
Hw 203										
CASA AZ	41.27	37.643611	118.908056	331654	4167780	37.64353	-118.90907	2209.634	2211.173	0.004
DBR15	41.53	37.642778	118.910556	331432	4167696	37.64273	-118.91157	2215.042	2216.579	0.005
DBR16	41.58							2218.106	2219.890	0.005
DBR17	41.63	37.642222	118.911389	331360	4167631	37.64213	-118.91237	2220.713	2222.248	0.005
DBR19	41.77	37.641944	118.913056	331209	4167601	37.64183	-118.91407	2227.385	2228.921	0.005
DBR20	41.82	37.641667	118.913889	331138	4167580	37.64163	-118.91487	2229.134	2230.670	0.005
DBR21	41.86	37.641389	118.914444	331093	4167548	37.64133	-118.91537	2230.209	2231.746	0.005
1LRM	42.48	37.640000	118.920556	330543	4167404	37.63993	-118.92157	2239.175	2240.724	0.005
34EGE	42.58	37.640278	118.921111	330500	4167438	37.64023	-118.92207	2242.761	2244.311	0.005
35EGE	43.6	37.639167	118.932222	329518	4167336	37.63913	-118.93317	2288.375	2289.941	0.005
36EGE	43.88	37.639167	118.935000	329271	4167341	37.63913	-118.93597	2300.971	2302.537	0.005
37EGE	44.22	37.640000	118.938611	328955	4167436	37.63993	-118.93957	2316.878	2318.445	0.005
38EGE	44.43	37.640833	118.940278	328807	4167528	37.64073	-118.94127	2326.490	2328.057	0.005
2JCM	44.68	37.641667	118.940278	328809	4167628	37.64163	-118.94127	2331.964	2333.530	0.005
39EGE	44.98	37.643056	118.945278	328371	4167792	37.64303	-118.94627	2332.273	2333.844	0.005
3LRM	45.79	37.646111	118.953056	327689	4168140	37.64603	-118.95407	2357.627	2359.202	0.005
STA907	45.88	37.646111	118.953611	327645	4168141	37.64603	-118.95457	2357.469	2359.046	0.005
3JCM	46.4	37.647500	118.958611	327207	4168305	37.64743	-118.95957	2373.041	2374.622	0.005
K1383	47.49	37.648333	118.970556	326150	4168416	37.64823	-118.97157	2395.076	2396.670	0.005
J1383	48.54	37.648611	118.981944	325154	4168470	37.64854	-118.98287	2444.373	2445.984	0.005
H1383	49.39	37.653611	118.986944	324725	4169034	37.65353	-118.98787	2473.767	2475.391	0.005
5JCM	49.95	37.656111	118.991389	324334	4169320	37.65603	-118.99237	2505.020	2506.653	0.005
G1383	50.69	37.653611	118.994167	324081	4169048	37.65354	-118.99517	2545.448	2547.083	0.005
F1383	51.42	37.650556	118.999167	323633	4168725	37.65054	-119.00017	2582.893	2584.539	0.005
6JCM	51.6	37.651667	119.000278	323538	4168849	37.65164	-119.00127	2596.167	2597.814	0.005
E1383	52.27	37.650833	119.006667	322971	4168761	37.65074	-119.00767	2632.094	2633.745	0.005
7JCM	52.82	37.648056	119.010833	322603	4168469	37.64804	-119.01177	2654.897	2656.551	0.005
8JCM	53.85	37.650000	119.021667	321646	4168701	37.64994	-119.02267	2690.411	2692.077	0.005
JEE17	55.07	37.653333	119.032778	320675	4169088	37.65324	-119.03377	2688.590	2690.272	0.005
PM14	55.57			320472	4168980	37.65222	-119.03604	2705.347	2707.054	0.005
9JCM	55.66	37.651667	119.037778	320230	4168920	37.65164	-119.03877	2715.027	2716.705	0.005
PM15	55.77							2724.494	2726.198	0.005
42EGE	56.88	37.651667	119.050833	319083	4168945	37.65164	-119.05177	2759.282	2760.943	0.005

Table 1. Leveling heights for the Long Valley region (see fig. 1B for bench mark locations)—Continued.

BM ID	Distance	NAD 27				NAD 83		2006 leveling heights (m)		
		LAT (°)	W LONG (°)	X (UTM)	Y (UTM)	LAT (°)	LONG (°)	raw	ortho	σ
D1383	57.68	37.654167	119.056667	318568	4169234	37.65414	-119.05767	2796.339	2797.979	0.005
20JD	57.73	37.654167	119.056944	318551	4169234	37.65414	-119.05787	2796.461	2798.097	0.005
RET	58.11	37.656667	119.059722	318310	4169517	37.65664	-119.06067	2823.587	2825.176	0.005
Antelope Valley Rd										
3EGE	39.73	37.652500	118.921111	330527	4168791	37.65243	-118.92207	2230.089	2231.641	0.004
12EGE	40.01	37.654167	118.918611	330752	4168976	37.65413	-118.91957	2236.042	2237.591	0.004
13EGE	40.28	37.651944	118.916111	330967	4168716	37.65183	-118.91707	2249.094	2250.638	0.004
24JCM	40.55	37.654167	118.914722	331096	4168969	37.65413	-118.91567	2272.126	2273.669	0.004
14EGE	40.96	37.655833	118.914444	331126	4169146	37.65573	-118.91537	2276.599	2278.144	0.004
15EGE	41.27	37.657500	118.911111	331421	4169328	37.65743	-118.91207	2289.307	2290.857	0.004
16EGE	41.95	37.660000	118.909722	331550	4169603	37.65993	-118.91067	2307.087	2308.640	0.005
23JCM	42.01	37.664167	118.906667	331824	4170064	37.66413	-118.90767	2328.435	2329.995	0.005
17EGE	42.27	37.664167	118.906667	331824	4170064	37.66413	-118.90767	2338.736	2340.294	0.005
18EGE	42.67	37.666111	118.906389	331855	4170274	37.66603	-118.90737	2327.664	2329.226	0.005
19EGE	42.96	37.668889	118.904167	332055	4170581	37.66883	-118.90517	2330.719	2332.285	0.005
20EGE	43.22	37.671389	118.903611	332114	4170857	37.67133	-118.90457	2336.381	2337.947	0.005
22JCM	43.83	37.673333	118.902500	332215	4171066	37.67323	-118.90347	2340.491	2342.057	0.005
22EGE	44.14	37.674722	118.899722	332465	4171216	37.67463	-118.90067	2340.094	2341.661	0.005
23EGE	44.53	37.675000	118.897222	332687	4171245	37.67493	-118.89817	2343.340	2344.906	0.005
21JCM	44.83	37.674167	118.893889	332976	4171150	37.67413	-118.89487	2326.433	2328.001	0.005
24EGE	45.23	37.673333	118.890556	333265	4171045	37.67323	-118.89157	2320.305	2321.872	0.005
25EGE	45.57	37.673611	118.886944	333592	4171071	37.67353	-118.88787	2301.172	2302.739	0.005
26EGE	45.94	37.676111	118.886667	333615	4171348	37.67603	-118.88767	2279.865	2281.432	0.005
27EGE	46.27	37.679167	118.885833	333701	4171691	37.67913	-118.88677	2256.428	2257.992	0.005
KWH5	47.12	37.679167	118.877778	334407	4171677	37.67913	-118.87877	2198.973	2200.516	0.005
KWH6	47.17	37.679167	118.877222	334460	4171676	37.67913	-118.87817	2199.125	2200.666	0.005
18JCM RESET	47.75	37.681944	118.871944	334933	4171966	37.68183	-118.87287	2202.042	2203.568	0.005
25JCM	49.36	37.687222	118.858889	336091	4172531	37.68713	-118.85987	2211.396	2212.922	0.005
26JCM	50.99	37.683611	118.841389	337627	4172101	37.68353	-118.84237	2157.287	2158.812	0.005
27JCM	52.3	37.679722	118.828333	338774	4171646	37.67963	-118.82927	2128.954	2130.478	0.005
28JCM RESET	53.19	37.676667	118.819167	339570	4171297	37.67663	-118.82016	2122.305	2123.831	0.005
43DOR	54.49	37.684167	118.810556	340344	4172115	37.68413	-118.81156	2111.871	2113.400	0.005
44DOR	55.79	37.675000	118.805833	340748	4171086	37.67493	-118.80676	2120.750	2122.281	0.005
29JCM	55.85	37.675000	118.805278	340792	4171085	37.67493	-118.80626	2123.125	2124.655	0.005
Long Valley										
43DOR	54.49	37.684167	118.810556	340344	4172115	37.68413	-118.81156	2111.871	2113.400	0.005

Table 1. Leveling heights for the Long Valley region (see fig. 1B for bench mark locations)—Continued.

BM ID	Distance	NAD 27				NAD 83		2006 leveling heights (m)		
		LAT (°)	W LONG (°)	X (UTM)	Y (UTM)	LAT (°)	LONG (°)	raw	ortho	σ
44DOR	55.79	37.675000	118.805833	340748	4171086	37.67493	-118.80676	2120.750	2122.281	0.005
29JCM	55.879	37.675000	118.805278	340792	4171085	37.67493	-118.80626	2123.125	2124.655	0.005
49DOR	57.094	37.685556	118.798333	341432	4172249	37.68553	-118.79926	2117.673	2119.201	0.005
T3S R29E	58.191	37.687500	118.789167	342238	4172445	37.68743	-118.79016	2098.894	2100.422	0.005
3JD	58.359	37.688333	118.787778	342363	4172531	37.68823	-118.78876	2108.117	2109.642	0.005
50DOR	59.832	37.687778	118.772778	343685	4172450	37.68773	-118.77376	2080.458	2081.980	0.005
4JD	61.963	37.699444	118.762222	344644	4173720	37.69933	-118.76316	2077.896	2079.386	0.006

Table 2. Long Valley region GPS-on-Bench Mark survey for 2006 (<http://quake.wr.usgs.gov/research/deformation/gps/auto/MammothLevel/index.html>).

BM ID	ITRF00							NAD83			
	X (m)	Y (m)	Z (m)	LAT (dms)	LONG (dms)	height (m)	σ (m)	LAT (dd)	LONG (dd)	height (m)	σ (m)
Hw 395											
C916	-2450419.145	-4401717.603	3901862.070	37 56 40.7939	-119 6 16.2618	2048.888	0.018	37.94466	-119.10450	2049.495	0.018
JUCT	-2451311.907	-4405770.894	3896805.613	37 53 12.2367	-119 5 27.5163	2078.324	0.018	37.88673	-119.09096	2078.932	0.018
BM07	-2451833.960	-4409032.959	3893006.686	37 50 33.2118	-119 4 41.3230	2197.436	0.013	37.84255	-119.07813	2198.046	0.013
T2SR	-2449570.806	-4415305.648	3887707.705	37 46 50.3230	-119 1 15.9916	2412.830	0.015	37.78064	-119.02109	2413.442	0.015
X123	-2447236.056	-4419592.030	3884073.818	37 44 25.2129	-118 58 27.7323	2256.680	0.017	37.74033	-118.97436	2257.295	0.017
EA15	-2446539.834	-4422417.572	3881355.677	37 42 33.1483	-118 57 7.0136	2282.240	0.018	37.70920	-118.95193	2282.856	0.018
D916	-2446675.900	-4422826.693	3880817.210	37 42 10.9301	-118 57 3.7904	2288.246	0.018	37.70303	-118.95104	2288.863	0.018
13DO	-2446236.824	-4424196.403	3879538.797	37 41 18.5810	-118 56 21.0628	2286.816	0.019	37.68849	-118.93917	2287.433	0.019
1EGE	-2446147.210	-4426593.686	3876751.808	37 39 26.3398	-118 55 30.5551	2209.887	0.021	37.65731	-118.92514	2210.505	0.021
A124	-2442387.554	-4430783.175	3874244.940	37 37 45.3173	-118 51 53.7879	2144.692	0.018	37.62925	-118.86493	2145.312	0.018
CONV	-2438694.463	-4433914.285	3872968.372	37 36 53.5008	-118 48 40.3435	2126.971	0.013	37.61486	-118.81119	2127.593	0.013
V911	-2438236.020	-4435715.037	3871102.288	37 35 38.7132	-118 47 48.6101	2063.397	0.020	37.59408	-118.79682	2064.020	0.020
D124	-2436073.169	-4438579.376	3869234.977	37 34 21.6729	-118 45 35.1857	2088.882	0.012	37.57268	-118.75976	2089.505	0.012
CROA	-2432179.496	-4441819.302	3868009.583	37 33 31.0159	-118 42 12.6637	2110.124	0.020	37.57268	-118.75976	2110.749	0.020
Hw 203											
2JCM	-2448139.275	-4426795.549	3875434.378	37 38 29.9317	-118 56 37.6672	2308.123	0.018	37.64164	-118.94378	2308.740	0.018
K138	-2450061.872	-4425273.250	3876057.839	37 38 53.8817	-118 58 16.3161	2371.290	0.026	37.64830	-118.97118	2371.907	0.026
5JCM	-2451481.682	-4423984.601	3876807.417	37 39 21.8251	-118 59 32.4275	2481.347	0.042	37.65606	-118.99233	2481.963	0.042
PM14	-2455059.681	-4422479.395	3876592.227	37 39 8.0001	-119 2 9.7977	2681.712	0.020	37.65222	-119.03604	2682.327	0.020
RETT	-2456867.244	-4421287.068	3876999.297	37 39 21.7108	-119 3 37.8439	2800.002	0.013	37.65603	-119.06050	2800.616	0.013
Antelope Valley Rd											
18EG	-2444518.478	-4426901.440	3877576.656	37 39 57.7769	-118 54 26.3383	2303.678	0.029	37.66605	-118.90730	2304.296	0.029
25EG	-2442785.387	-4427263.227	3878207.757	37 40 24.2927	-118 53 17.3162	2277.133	0.021	37.67341	-118.88813	2277.751	0.021
KWH6	-2441775.218	-4427266.572	3878668.793	37 40 45.7358	-118 52 41.1673	2175.047	0.019	37.67937	-118.87809	2175.665	0.019
25JC	-2440123.372	-4427570.743	3879376.437	37 41 14.4222	-118 51 36.1584	2187.269	0.022	37.68734	-118.86003	2187.888	0.022
26JC	-2438889.595	-4428453.656	3879057.484	37 41 2.7103	-118 50 34.6865	2133.127	0.019	37.68408	-118.84295	2133.746	0.019
44DO	-2436384.951	-4430499.056	3878240.950	37 40 30.1741	-118 48 24.9339	2096.536	0.016	37.67504	-118.80691	2097.156	0.016
29JC	-2436349.096	-4430535.028	3878226.400	37 40 29.5184	-118 48 22.9451	2098.917	0.018	37.67486	-118.80636	2099.537	0.018
Long Valley											
T3SR	-2434676.129	-4430438.460	3879339.680	37 41 15.7376	-118 47 25.0312	2074.636	0.020	37.68770	-118.79027	2075.256	0.020
4JDD	-2432186.508	-4430876.515	3880359.537	37 41 58.0532	-118 45 47.3840	2053.676	0.019	37.69946	-118.76315	2054.296	0.019

Table 3. Experimental hybrid geoid height (N+s) for the Long Valley region.

BM ID	Distance	UTM NAVD 27		NAD83 GPS		NAVD88 leveled		measured geoid		GEOID03		Geoids difference	
		X	Y	height (m)	σ (m)	height (m)	σ (m)	N+s (m)	σ (m)	N+s (m)	σ (m)	Δ (m)	σ (m)
Hw 395													
C916	0	315132	4201661	2049.495	0.018	2073.909	0.000	-24.414	0.018	-24.408	0.024	-0.006	0.030
JUCTION	7.22	316233	4195097	2078.932	0.018	2103.324	0.002	-24.392	0.018	-24.374	0.024	-0.018	0.030
BM7	12.29	317197	4190169	2198.046	0.013	2222.401	0.002	-24.355	0.013	-24.364	0.024	0.009	0.027
T2SR	21.91	322099	4183201	2413.442	0.015	2438.180	0.003	-24.738	0.015	-24.454	0.024	-0.284	0.028
X123	28.29	326127	4178629	2257.295	0.017	2281.984	0.004	-24.689	0.017	-24.624	0.024	-0.065	0.030
EAL15	32.37	328038	4175137	2282.856	0.018	2307.738	0.004	-24.882	0.018	-24.750	0.024	-0.132	0.030
D916	33.09	328095	4174459	2288.863	0.018	2313.766	0.004	-24.903	0.018	-24.754	0.024	-0.149	0.030
13DOR	35.25	329092	4172773	2287.433	0.019	2312.335	0.004	-24.902	0.019	-24.778	0.024	-0.124	0.031
1EGE	39.12	330291	4169318	2210.505	0.021	2235.359	0.004	-24.854	0.021	-24.749	0.024	-0.105	0.032
A124 RESET	46.04	335576	4166125	2145.312	0.018	2170.171	0.005	-24.859	0.019	-24.723	0.024	-0.136	0.030
CONVICT	51.16	340248	4164402	2127.593	0.013	2152.398	0.005	-24.805	0.014	-24.727	0.024	-0.078	0.028
V911	53.87	341581	4162068	2064.020	0.020	2088.710	0.005	-24.690	0.021	-24.608	0.024	-0.082	0.032
D124	57.99	344672	4159701	2089.505	0.012	2114.139	0.005	-24.634	0.013	-24.558	0.024	-0.076	0.027
CROWLEY AZ	64.05	349651	4158000	2110.749	0.020	2135.442	0.006	-24.693	0.021	-24.662	0.024	-0.031	0.032
Hw 203													
2JCM	44.68	328809	4167628	2308.740	0.018	2333.530	0.005	-24.790	0.019	-24.668	0.024	-0.122	0.030
K1383	47.49	326150	4168416	2371.907	0.026	2396.670	0.005	-24.763	0.026	-24.657	0.024	-0.106	0.036
5JCM	49.95	324334	4169320	2481.963	0.042	2506.653	0.005	-24.690	0.042	-24.651	0.024	-0.039	0.049
PM14	55.57	320472	4168980	2682.327	0.020	2707.054	0.005	-24.727	0.021	-24.593	0.024	-0.134	0.032
RET	58.11	318310	4169517	2800.616	0.013	2825.176	0.005	-24.560	0.014	-24.543	0.024	-0.017	0.028
Antelope V.													
18EGE	42.67	331855	4170274	2304.296	0.029	2329.226	0.005	-24.930	0.029	-24.808	0.024	-0.122	0.038
25EGE	45.57	333592	4171071	2277.751	0.021	2302.739	0.005	-24.988	0.022	-24.851	0.024	-0.137	0.032
KWH6	47.17	334460	4171676	2175.665	0.019	2200.666	0.005	-25.001	0.020	-24.866	0.024	-0.135	0.031
25JCM	49.36	336091	4172531	2187.888	0.022	2212.922	0.005	-25.034	0.023	-24.899	0.024	-0.135	0.033
26JCM	50.99	337627	4172101	2133.746	0.019	2158.812	0.005	-25.066	0.020	-24.923	0.024	-0.143	0.031
44DOR	55.79	340748	4171086	2097.156	0.016	2122.281	0.005	-25.125	0.017	-24.962	0.024	-0.163	0.029
29JCM	55.85	340792	4171085	2099.537	0.018	2124.655	0.005	-25.118	0.019	-24.962	0.024	-0.156	0.030
Long Valley													
T3S R29E	58.191	342238	4172445	2075.256	0.020	2100.422	0.005	-25.166	0.021	-24.981	0.024	-0.185	0.032
4JD	61.963	344644	4173720	2054.296	0.019	2079.386	0.006	-25.090	0.020	-24.959	0.024	-0.131	0.031

Table 4. Experimental conversion surface s for the Long Valley region.

BM ID	NAD83 GPS		NAVD88 leveled		USGG2003		s	
	height (m)	σ (m)	height (m)	σ (m)	height (m)	height (m)	σ (m)	
Hw 395								
C916	2049.495	0.018	2073.909	0.000	-24.320	-0.094	0.024	
JUCTION	2078.932	0.018	2103.324	0.002	-24.299	-0.093	0.024	
BM7	2198.046	0.013	2222.401	0.002	-24.300	-0.055	0.024	
T2SR ¹	2413.442	0.015	2438.180	0.003	-24.419	-0.319	0.024	
X123	2257.295	0.017	2281.984	0.004	-24.610	-0.079	0.024	
EAL15	2282.856	0.018	2307.738	0.004	-24.749	-0.133	0.024	
D916	2288.863	0.018	2313.766	0.004	-24.755	-0.148	0.024	
13DOR	2287.433	0.019	2312.335	0.004	-24.785	-0.117	0.024	
1EGE	2210.505	0.021	2235.359	0.004	-24.767	-0.087	0.024	
A124 RESET	2145.312	0.018	2170.171	0.005	-24.762	-0.097	0.024	
CONVICT	2127.593	0.013	2152.398	0.005	-24.776	-0.029	0.024	
V911	2064.020	0.020	2088.710	0.005	-24.663	-0.027	0.024	
D124	2089.505	0.012	2114.139	0.005	-24.620	-0.014	0.024	
CROWLEY AZ	2110.749	0.020	2135.442	0.006	-24.730	0.037	0.024	
Hw 203								
2JCM	2308.740	0.018	2333.530	0.005	-24.686	-0.104	0.024	
K1383	2371.907	0.026	2396.670	0.005	-24.665	-0.098	0.024	
5JCM	2481.963	0.042	2506.653	0.005	-24.652	-0.038	0.024	
PM14 ¹	2682.327	0.020	2707.054	0.005	-24.584	-0.143	0.024	
RET	2800.616	0.013	2825.176	0.005	-24.527	-0.033	0.024	
Antelope V.								
18EGE	2304.296	0.029	2329.226	0.005	-24.828	-0.102	0.024	
25EGE	2277.751	0.021	2302.739	0.005	-24.873	-0.115	0.024	
KWH6	2175.665	0.019	2200.666	0.005	-24.889	-0.112	0.024	
25JCM	2187.888	0.022	2212.922	0.005	-24.925	-0.109	0.024	
26JCM	2133.746	0.019	2158.812	0.005	-24.954	-0.112	0.024	
44DOR	2097.156	0.016	2122.281	0.005	-25.001	-0.124	0.024	
29JCM	2099.537	0.018	2124.655	0.005	-25.001	-0.117	0.024	
Long Valley								
T3S R29E	2075.256	0.020	2100.422	0.005	-25.021	-0.145	0.024	
4JD	2054.296	0.019	2079.386	0.006	-25.001	-0.089	0.024	

¹ This point is an outlier and has not been included in the final interpolation.

Table 5. Geoid heights at leveling benchmarks for the Long Valley region (see fig. 1B for benchmark location).

BM	UTM NAD27		LVGEOID (m)		Conversion surface s (m)		USGG2003 height (m)
	X	Y	height	σ	height	σ	
LINE 1: HIGHWAY 395							
F124	350193	4158179	-24.721	0.028	0.038	0.027	-24.759
CROWLEY AZ ¹	349651	4158000	-24.693	0.021	0.037	0.000	-24.73
P911	348423	4158055	-24.654	0.030	0.027	0.030	-24.681
P911 RESET	348418	4157745	-24.638	0.027	0.028	0.027	-24.666
E124	347595	4158659	-24.662	0.029	0.016	0.029	-24.678
C1433	346442	4158425	-24.619	0.030	0.007	0.030	-24.626
BMQ	346317	4158371	-24.613	0.029	0.006	0.029	-24.619
Q911	346128	4158619	-24.617	0.028	0.003	0.029	-24.62
D124 ¹	344672	4159701	-24.634	0.013	-0.014	0.000	-24.62
U911	343683	4160674	-24.665	0.031	-0.020	0.031	-24.645
C124	342588	4161150	-24.656	0.029	-0.023	0.030	-24.633
6DOR	342545	4161184	-24.658	0.029	-0.024	0.030	-24.634
V911 ¹	341581	4162068	-24.690	0.021	-0.027	0.000	-24.663
B124	340910	4163002	-24.727	0.029	-0.027	0.029	-24.7
7DOR	340789	4163160	-24.733	0.030	-0.027	0.030	-24.706
CONVICT ¹	340248	4164402	-24.805	0.014	-0.029	0.000	-24.776
8DOR	339180	4164856	-24.822	0.031	-0.044	0.031	-24.778
T911 RESET	338425	4165115	-24.833	0.030	-0.056	0.030	-24.777
9DOR	337742	4165406	-24.845	0.029	-0.067	0.029	-24.778
9DOR RESET	337742	4165406	-24.845	0.029	-0.067	0.029	-24.778
S911 RESET	336892	4165700	-24.854	0.028	-0.080	0.028	-24.774
A124	335522	4166104	-24.857	0.000	-0.097	0.019	-24.76
A124 RESET ¹	335576	4166125	-24.859	0.019	-0.097	0.000	-24.762
10DOR	334524	4166524	-24.857	0.021	-0.101	0.021	-24.756
R911	334603	4166456	-24.854	0.021	-0.100	0.021	-24.754
11DOR	333018	4167142	-24.848	0.021	-0.099	0.021	-24.749
MGB13	332965	4167110	-24.844	0.021	-0.098	0.021	-24.746
MGB14	332895	4167145	-24.843	0.020	-0.097	0.020	-24.746
MGB16	332852	4167201	-24.845	0.020	-0.097	0.020	-24.748
MGB17	332773	4167236	-24.844	0.021	-0.096	0.022	-24.748
11EGE	332730	4167270	-24.844	0.021	-0.096	0.022	-24.748
MGB18	332677	4167294	-24.844	0.022	-0.096	0.022	-24.748
MGB19	332651	4167294	-24.843	0.022	-0.096	0.022	-24.747
MGB20	332581	4167329	-24.843	0.022	-0.096	0.022	-24.747
MGB21	332528	4167330	-24.842	0.022	-0.096	0.022	-24.746
10EGE	332335	4167400	-24.841	0.022	-0.096	0.022	-24.745
9EGE	332145	4167582	-24.848	0.020	-0.096	0.020	-24.752
DBR1	332143	4167493	-24.841	0.020	-0.096	0.020	-24.745
DBR2	332117	4167527	-24.842	0.021	-0.096	0.021	-24.746
DBR3	332047	4167562	-24.842	0.021	-0.096	0.021	-24.746
DBR4	331995	4167585	-24.844	0.021	-0.095	0.021	-24.749
DBR5	331978	4167619	-24.845	0.020	-0.095	0.020	-24.75
8EGE	331952	4167686	-24.847	0.020	-0.095	0.020	-24.752
DBR6	331925	4167620	-24.844	0.020	-0.095	0.020	-24.749
DBR7	331873	4167687	-24.845	0.021	-0.095	0.021	-24.75
DBR8	331830	4167721	-24.846	0.021	-0.095	0.021	-24.751
DBR9	331759	4167745	-24.845	0.021	-0.095	0.021	-24.75
DBR10	331707	4167779	-24.842	0.019	-0.095	0.019	-24.747

Table 5. Geoid heights at leveling benchmarks for the Long Valley region (see fig. 1B for benchmark location)—Continued.

BM	UTM NAD27		LVGEOID (m)		Conversion surface s (m)		USGG2003
	X	Y	height	σ	height	σ	height (m)
DBR11	331637	4167814	-24.842	0.021	-0.095	0.022	-24.747
CASA AZ	331654	4167780	-24.841	0.019	-0.095	0.019	-24.746
7EGE	331419	4167907	-24.839	0.022	-0.094	0.022	-24.745
Z123	331200	4168034	-24.837	0.021	-0.093	0.021	-24.744
6EGE	331052	4168137	-24.838	0.020	-0.093	0.020	-24.745
5EGE	330862	4168296	-24.838	0.021	-0.092	0.021	-24.746
4EGE	330673	4168578	-24.843	0.021	-0.091	0.021	-24.752
3EGE	330527	4168791	-24.845	0.020	-0.089	0.020	-24.756
2EGE	330383	4169072	-24.850	0.018	-0.088	0.019	-24.762
1EGE ¹	330291	4169318	-24.854	0.021	-0.087	0.000	-24.767
W911	330131	4169699	-24.863	0.018	-0.089	0.019	-24.774
BM12	329714	4170873	-24.886	0.013	-0.099	0.013	-24.787
X911	329346	4171003	-24.882	0.014	-0.101	0.014	-24.781
12DOR	329559	4171897	-24.901	0.014	-0.108	0.014	-24.793
13DOR ¹	329092	4172773	-24.902	0.019	-0.117	0.000	-24.785
Y123	328821	4172901	-24.902	0.013	-0.121	0.013	-24.781
14DOR	328464	4173552	-24.905	0.014	-0.135	0.014	-24.77
Z1382	328371	4173742	-24.905	0.014	-0.138	0.014	-24.767
Z1382 RESET	328371	4173742	-24.905	0.014	-0.138	0.014	-24.767
D916 ¹	328095	4174459	-24.903	0.018	-0.148	0.000	-24.755
EAL33	328124	4174602	-24.901	0.013	-0.146	0.013	-24.755
EAL15 ¹	328038	4175137	-24.882	0.018	-0.133	0.000	-24.749
B13	327780	4175875	-24.854	0.014	-0.123	0.014	-24.731
69.97RT	327524	4176280	-24.830	0.014	-0.116	0.014	-24.714
Y911	327259	4176696	-24.797	0.014	-0.109	0.014	-24.688
Z911	326554	4177965	-24.730	0.017	-0.089	0.017	-24.641
15DOR	326407	4178102	-24.718	0.019	-0.086	0.019	-24.632
X123 ¹	326127	4178629	-24.689	0.017	-0.079	0.000	-24.61
CRESTVIEW	326127	4178629	-24.689	0.000	-0.079	0.017	-24.61
A1383	325864	4179090	-24.662	0.023	-0.076	0.023	-24.586
CAL TRAN88	325591	4179962	-24.632	0.025	-0.072	0.025	-24.56
L916	325345	4179967	-24.621	0.026	-0.070	0.026	-24.551
L916 RESET	325345	4179967	-24.621	0.026	-0.070	0.026	-24.551
B1383	324754	4180812	-24.593	0.028	-0.069	0.028	-24.524
KUSE	324365	4181165	-24.570	0.028	-0.067	0.028	-24.503
A1391	323996	4181228	-24.555	0.030	-0.065	0.030	-24.49
B1391	323687	4181612	-24.539	0.029	-0.064	0.029	-24.475
BM2	323160	4182078	-24.517	0.030	-0.062	0.030	-24.455
T2SR	322099	4183201	-24.478	0.033	-0.059	0.033	-24.419
K916	322160	4183121	-24.481	0.032	-0.060	0.032	-24.421
16DOR	321303	4184250	-24.447	0.034	-0.057	0.034	-24.39
J916	320624	4185841	-24.429	0.033	-0.056	0.033	-24.373
H916	320553	4185809	-24.426	0.034	-0.055	0.034	-24.371
BM5	319470	4186632	-24.401	0.034	-0.053	0.034	-24.348
5 RESET	319470	4186632	-24.401	0.034	-0.053	0.034	-24.348
BM6	318614	4187762	-24.378	0.032	-0.052	0.032	-24.326
M916	317759	4188924	-24.360	0.029	-0.052	0.029	-24.308
BM7 ¹	317197	4190169	-24.355	0.013	-0.055	0.000	-24.3
N916	316757	4191378	-24.356	0.030	-0.064	0.030	-24.292

Table 5. Geoid heights at leveling benchmarks for the Long Valley region (see fig. 1B for benchmark location)—Continued.

BM	UTM NAD27		LVGEOID (m)		Conversion surface s (m)		USGG2003 height (m)
	X	Y	height	σ	height	σ	
W123	316514	4192316	-24.360	0.030	-0.071	0.030	-24.289
W123 RESET	316421	4192495	-24.359	0.030	-0.073	0.030	-24.286
R916	316393	4193584	-24.376	0.028	-0.082	0.028	-24.294
JUCTION ¹	316233	4195097	-24.392	0.018	-0.093	0.000	-24.299
V123	316045	4195313	-24.385	0.026	-0.093	0.026	-24.292
DIABLO	316060	4196023	-24.394	0.026	-0.095	0.026	-24.299
DIABLO RESET	316060	4196023	-24.394	0.026	-0.095	0.026	-24.299
Q916	315869	4197293	-24.397	0.028	-0.095	0.028	-24.302
P916	315774	4198560	-24.407	0.028	-0.095	0.028	-24.312
U123	315350	4200413	-24.407	0.024	-0.094	0.024	-24.313
C916 ¹	315132	4201661	-24.414	0.018	-0.094	0.000	-24.32
LINE 2: HIGHWAY 203							
CASA AZ	331654	4167780	-24.841	0.019	-0.095	0.019	-24.746
DBR11	331637	4167814	-24.842	0.021	-0.095	0.022	-24.747
DBR12	331584	4167782	-24.839	0.019	-0.095	0.019	-24.744
DBR13	331512	4167750	-24.836	0.021	-0.095	0.021	-24.741
DBR14	331485	4167728	-24.835	0.021	-0.095	0.021	-24.74
DBR15	331432	4167696	-24.832	0.021	-0.095	0.021	-24.737
DBR17	331360	4167631	-24.828	0.021	-0.095	0.021	-24.733
DBR18	331289	4167599	-24.825	0.022	-0.095	0.022	-24.73
DBR19	331209	4167601	-24.823	0.022	-0.095	0.022	-24.728
DBR20	331138	4167580	-24.820	0.022	-0.095	0.022	-24.725
DBR21	331093	4167548	-24.818	0.020	-0.095	0.020	-24.723
33EGE	330819	4167520	-24.812	0.021	-0.095	0.021	-24.717
1LRM	330543	4167404	-24.803	0.021	-0.096	0.021	-24.707
34EGE	330500	4167438	-24.803	0.022	-0.096	0.022	-24.707
1JCM	330084	4167380	-24.795	0.021	-0.097	0.022	-24.698
2LRM	329712	4167332	-24.789	0.021	-0.099	0.021	-24.69
35EGE	329518	4167336	-24.787	0.022	-0.100	0.022	-24.687
36EGE	329271	4167341	-24.784	0.019	-0.101	0.019	-24.683
37EGE	328955	4167436	-24.784	0.020	-0.103	0.020	-24.681
38EGE	328807	4167528	-24.786	0.019	-0.104	0.019	-24.682
2JCM ¹	328809	4167628	-24.790	0.019	-0.104	0.000	-24.686
39EGE	328371	4167792	-24.790	0.018	-0.104	0.018	-24.686
40EGE	328084	4168009	-24.791	0.021	-0.104	0.021	-24.687
3LRM	327689	4168140	-24.788	0.023	-0.104	0.023	-24.684
STA907	327645	4168141	-24.788	0.023	-0.104	0.023	-24.684
41EGE	327374	4168235	-24.786	0.020	-0.104	0.020	-24.682
3JCM	327207	4168305	-24.785	0.021	-0.103	0.021	-24.682
K1383 ¹	326150	4168416	-24.763	0.026	-0.098	0.000	-24.665
4JCM	325038	4168839	-24.714	0.024	-0.062	0.024	-24.652
J1383	325154	4168470	-24.714	0.026	-0.069	0.026	-24.645
H1383	324725	4169034	-24.702	0.027	-0.051	0.027	-24.651
5JCM ¹	324334	4169320	-24.690	0.042	-0.038	0.000	-24.652
G1383	324081	4169048	-24.681	0.028	-0.038	0.028	-24.643
F1383	323633	4168725	-24.669	0.030	-0.037	0.030	-24.632
6JCM	323538	4168849	-24.669	0.029	-0.036	0.029	-24.633
E1383	322971	4168761	-24.659	0.031	-0.034	0.031	-24.625

Table 5. Geoid heights at leveling benchmarks for the Long Valley region (see fig. 1B for benchmark location)—Continued.

BM	UTM NAD27		LVGEOID (m)		Conversion surface s (m)		USGG2003 height (m)
	X	Y	height	σ	height	σ	
7JCM	322603	4168469	-24.658	0.032	-0.034	0.032	-24.624
8JCM	321646	4168701	-24.642	0.033	-0.032	0.033	-24.61
JEE1	321481	4168826	-24.637	0.033	-0.032	0.033	-24.605
JEE3	321307	4168952	-24.629	0.032	-0.032	0.032	-24.597
JEE6	321142	4169078	-24.623	0.032	-0.032	0.032	-24.591
JEE9	320979	4169270	-24.615	0.032	-0.032	0.032	-24.583
JEE12	320871	4169184	-24.616	0.031	-0.032	0.031	-24.584
JEE15	320772	4169119	-24.616	0.031	-0.032	0.031	-24.584
JEE17	320675	4169088	-24.616	0.032	-0.032	0.032	-24.584
JEE19	320576	4169035	-24.616	0.032	-0.032	0.032	-24.584
JEE20	320479	4169003	-24.616	0.032	-0.032	0.032	-24.584
JEE22	320354	4168973	-24.615	0.032	-0.032	0.032	-24.583
PM14	320472	4168980	-24.616	0.032	-0.032	0.032	-24.584
9JCM	320230	4168920	-24.616	0.030	-0.032	0.030	-24.584
42EGE	319083	4168945	-24.605	0.032	-0.032	0.032	-24.573
D1383	318568	4169234	-24.583	0.031	-0.032	0.031	-24.551
20JD	318551	4169234	-24.582	0.031	-0.032	0.031	-24.55
RET ¹	318310	4169517	-24.560	0.014	-0.033	0.000	-24.527

LINE 3: LOOKOUT MTN-CASHBAUGH RANCH-WHITMORE HOT SPRINGS-CONVICT CREEK

8DOR	339180	4164856	-24.822	0.031	-0.044	0.031	-24.778
T911 RESET	338425	4165115	-24.833	0.030	-0.056	0.030	-24.777
9DOR RESET	337742	4165406	-24.845	0.029	-0.067	0.029	-24.778
1JD	340232	4166312	-24.934	0.028	-0.057	0.028	-24.877
48DOR	340225	4166867	-24.965	0.027	-0.065	0.026	-24.9
47DOR	340417	4168129	-25.026	0.020	-0.082	0.020	-24.944
46DOR	340781	4169143	-25.069	0.018	-0.095	0.018	-24.974
45DOR	340212	4170297	-25.093	0.014	-0.109	0.014	-24.984
2JD	340272	4170662	-25.102	0.013	-0.113	0.013	-24.989
29JCM ¹	340792	4171085	-25.121	0.019	-0.120	0.000	-25.001
44DOR ¹	340748	4171086	-25.121	0.017	-0.120	0.000	-25.001
43DOR	340344	4172115	-25.128	0.013	-0.126	0.013	-25.002
42DOR	340072	4173108	-25.127	0.014	-0.127	0.014	-25
41DOR	340380	4173957	-25.126	0.015	-0.127	0.015	-24.999
40DOR	340648	4175062	-25.107	0.017	-0.120	0.017	-24.987
39DOR	340138	4176492	-25.059	0.018	-0.112	0.018	-24.947
38DOR	339911	4177551	-25.015	0.021	-0.108	0.021	-24.907
26DOR	339094	4178144	-24.979	0.023	-0.106	0.023	-24.873
25DOR	337403	4178211	-24.957	0.020	-0.106	0.020	-24.851
24DOR	336407	4178663	-24.942	0.021	-0.127	0.021	-24.815
23DOR	334991	4178847	-24.891	0.023	-0.095	0.023	-24.796
G916	333534	4179120	-24.858	0.021	-0.094	0.021	-24.764
F916	331752	4179501	-24.813	0.020	-0.095	0.020	-24.718
NUSE	331505	4179506	-24.808	0.021	-0.095	0.020	-24.713
E916	329965	4179626	-24.771	0.020	-0.091	0.020	-24.68
MUSE	328750	4178852	-24.781	0.019	-0.095	0.020	-24.686
LUSE	327572	4177733	-24.796	0.016	-0.102	0.016	-24.694
69.97RT	327524	4176280	-24.830	0.014	-0.116	0.014	-24.714
B13	327780	4175875	-24.854	0.014	-0.123	0.014	-24.731

Table 5. Geoid heights at leveling benchmarks for the Long Valley region (see fig. 1B for benchmark location)—Continued.

BM	UTM NAD27		LVGEOD (m)		Conversion surface s (m)		USGG2003 height (m)
	X	Y	height	σ	height	σ	
LINE 4: CASHBAUGH RANCH-LITTLE ANTELOPE VALLEY-CASA							
29JCM ¹	340792	4171085	-25.121	0.019	-0.120	0.000	-25.001
44DOR ¹	340748	4171086	-25.121	0.017	-0.120	0.000	-25.001
43DOR	340344	4172115	-25.128	0.013	-0.126	0.013	-25.002
28JCM	339570	4171297	-25.102	0.014	-0.117	0.014	-24.985
28JCM RESET	339570	4171297	-25.102	0.014	-0.117	0.014	-24.985
27JCM	338774	4171646	-25.086	0.014	-0.115	0.014	-24.971
26JCM ¹	337627	4172101	-25.066	0.020	-0.112	0.000	-24.954
25JCM ¹	336091	4172531	-25.034	0.023	-0.109	0.000	-24.925
18JCM	334933	4171966	-25.012	0.013	-0.111	0.013	-24.901
18JCM RESET	334933	4171966	-25.012	0.013	-0.111	0.013	-24.901
KWH16	334854	4171967	-25.010	0.013	-0.111	0.013	-24.899
KWH15	334809	4171946	-25.010	0.013	-0.111	0.013	-24.899
KWH14	334782	4171880	-25.009	0.013	-0.111	0.013	-24.898
KWH13	334754	4171825	-25.008	0.013	-0.111	0.013	-24.897
KWH12	334727	4171792	-25.006	0.013	-0.111	0.013	-24.895
KWH11	334726	4171759	-25.005	0.013	-0.111	0.013	-24.894
KWH10	334709	4171759	-25.005	0.013	-0.111	0.013	-24.894
KWH9	334629	4171728	-25.004	0.013	-0.112	0.013	-24.892
KWH8	334558	4171729	-25.003	0.013	-0.112	0.013	-24.891
KWH7	334504	4171697	-25.002	0.000	-0.112	0.000	-24.89
KWH6 ¹	334460	4171676	-25.001	0.020	-0.112	0.000	-24.889
KWH5	334407	4171677	-25.000	0.000	-0.112	0.000	-24.888
KWH4	334381	4171699	-25.000	0.000	-0.112	0.000	-24.888
17JCM	333626	4171903	-24.996	0.013	-0.116	0.013	-24.88
27EGE	333701	4171691	-24.994	0.012	-0.115	0.012	-24.879
26EGE	333615	4171348	-24.989	0.013	-0.115	0.013	-24.874
25EGE ¹	333592	4171071	-24.988	0.022	-0.115	0.000	-24.873
24EGE	333265	4171045	-24.982	0.014	-0.114	0.014	-24.868
21JCM	332976	4171150	-24.980	0.012	-0.113	0.012	-24.867
23EGE	332687	4171245	-24.976	0.013	-0.112	0.013	-24.864
22EGE	332465	4171216	-24.970	0.014	-0.110	0.014	-24.86
21EGE	332465	4171216	-24.970	0.014	-0.110	0.014	-24.86
22JCM	332215	4171066	-24.961	0.013	-0.109	0.014	-24.852
20EGE	332114	4170857	-24.953	0.013	-0.107	0.014	-24.846
19EGE	332055	4170581	-24.944	0.014	-0.105	0.014	-24.839
18EGE ¹	331855	4170274	-24.928	0.029	-0.100	0.000	-24.828
17EGE	331824	4170064	-24.922	0.013	-0.100	0.013	-24.822
23JCM	331824	4170064	-24.922	0.013	-0.100	0.013	-24.822
16EGE	331550	4169603	-24.898	0.017	-0.096	0.017	-24.802
15EGE	331421	4169328	-24.886	0.018	-0.094	0.019	-24.792
14EGE	331126	4169146	-24.871	0.018	-0.091	0.018	-24.78
24JCM	331096	4168969	-24.865	0.019	-0.091	0.019	-24.774
13EGE	330967	4168716	-24.854	0.019	-0.091	0.019	-24.763
12EGE	330752	4168976	-24.855	0.019	-0.089	0.019	-24.766
3EGE	330527	4168791	-24.845	0.020	-0.089	0.020	-24.756

Table 5. Geoid heights at leveling benchmarks for the Long Valley region (see fig. 1B for benchmark location)—Continued.

BM	UTM NAD27		LVGEOID (m)		Conversion surface s (m)		USGG2003 height (m)
	X	Y	height	σ	height	σ	
LINE 5: SMOKEY BEAR FLAT-RESURGENT DOME-LITTLE ANTELOPE VALLEY							
17JCM	333626	4171903	-24.996	0.013	-0.116	0.013	-24.88
16PDI	333724	4171935	-24.996	0.012	-0.115	0.012	-24.881
15PDI	333804	4171988	-24.997	0.012	-0.114	0.012	-24.883
14PDI	333977	4172240	-25.002	0.013	-0.115	0.013	-24.887
4PDI	333886	4172542	-25.004	0.012	-0.116	0.012	-24.888
12PDI	333792	4172699	-25.005	0.013	-0.117	0.013	-24.888
31EGE	333797	4172954	-25.008	0.012	-0.118	0.012	-24.89
11PDI	333873	4173197	-25.013	0.013	-0.119	0.013	-24.894
10PDI	333753	4173355	-25.013	0.014	-0.120	0.014	-24.893
16JCM	333520	4173659	-25.014	0.014	-0.122	0.014	-24.892
9PDI	333400	4173817	-25.014	0.014	-0.123	0.014	-24.891
8PDI	333160	4174133	-25.006	0.015	-0.115	0.015	-24.891
32EGE	332914	4174204	-25.003	0.015	-0.116	0.015	-24.887
7PDI	332748	4174263	-25.001	0.015	-0.116	0.015	-24.885
15JCM	332779	4174485	-25.000	0.014	-0.116	0.014	-24.884
6PDI	332678	4174731	-24.997	0.013	-0.117	0.013	-24.88
5PDI	332585	4174921	-24.994	0.014	-0.118	0.014	-24.876
3PDI 1984	332567	4174922	-24.994	0.014	-0.118	0.014	-24.876
2PDI 1984	332420	4175047	-24.989	0.016	-0.118	0.016	-24.871
1PDI 1984	332231	4175295	-24.982	0.014	-0.119	0.014	-24.863
2PDI 1983	332110	4175419	-24.982	0.015	-0.124	0.015	-24.858
1PDI 1983	332088	4175631	-24.977	0.016	-0.124	0.016	-24.853
14JCM	332145	4175852	-24.962	0.016	-0.112	0.016	-24.85
13JCM	331088	4175907	-24.937	0.015	-0.115	0.015	-24.822
12JCM	330044	4175306	-24.931	0.014	-0.126	0.014	-24.805
L1383	330183	4174782	-24.943	0.013	-0.127	0.014	-24.816
11JCM	329670	4174726	-24.930	0.014	-0.130	0.014	-24.8
10JCM	329256	4173880	-24.922	0.013	-0.131	0.013	-24.791
13DOR	329092	4172773	-24.902	0.000	-0.117	0.000	-24.785
LINE 6: LAKE CROWLEY TIE A							
43DOR	340344	4172115	-25.128	0.013	-0.126	0.013	-25.002
44DOR	340748	4171086	-25.121	0.000	-0.120	0.000	-25.001
29JCM	340792	4171085	-25.121	0.000	-0.120	0.000	-25.001
49DOR	341432	4172249	-25.154	0.013	-0.140	0.013	-25.014
T3S R29E ¹	342238	4172445	-25.166	0.021	-0.145	0.000	-25.021
3JD	342363	4172531	-25.164	0.013	-0.143	0.013	-25.021
50DOR	343685	4172450	-25.136	0.015	-0.115	0.015	-25.021
4JD ¹	344644	4173720	-25.090	0.020	-0.089	0.000	-25.001
51DOR	345725	4172590	-25.087	0.024	-0.083	0.024	-25.004
52DOR	346806	4171404	-25.072	0.029	-0.074	0.029	-24.998
53DOR	347664	4170090	-25.052	0.031	-0.066	0.031	-24.986
54DOR	348132	4169160	-25.021	0.034	-0.048	0.034	-24.973
6JD	347895	4168243	-25.012	0.035	-0.045	0.035	-24.967
55DOR	348436	4166934	-24.971	0.037	-0.033	0.038	-24.938
56DOR	348436	4166934	-24.971	0.037	-0.033	0.038	-24.938
LC4B	348191	4167061	-24.978	0.036	-0.035	0.037	-24.943
LC4A	347697	4166582	-24.971	0.036	-0.035	0.036	-24.936

Table 5. Geoid heights at leveling benchmarks for the Long Valley region (see fig. 1B for benchmark location)—Continued.

BM	UTM NAD27		LVGEOID (m)		Conversion surface s (m)		USGG2003 height (m)
	X	Y	height	σ	height	σ	
TBM LC4	347495	4166208	-24.963	0.035	-0.034	0.035	-24.929
LINE 7: CONVICT LAKE SPUR							
9DOR RESET	337742	4165406	-24.845	0.029	-0.067	0.029	-24.778
30JCM	337210	4164373	-24.770	0.031	-0.064	0.031	-24.706
31JCM	336668	4163307	-24.678	0.031	-0.064	0.032	-24.614
32JCM	336621	4162253	-24.609	0.033	-0.063	0.033	-24.546
33JCM	336370	4161614	-24.555	0.034	-0.062	0.034	-24.493
LINE 8: DEADMAN SPUR							
EAL15	328038	4175137	-24.882	0.000	-0.133	0.000	-24.749
EAL3	328038	4175137	-24.882	0.000	-0.133	0.000	-24.749
34JCM	327392	4175028	-24.855	0.014	-0.129	0.014	-24.726
EAL1	327392	4175028	-24.855	0.014	-0.129	0.014	-24.726
35JCM	326049	4174923	-24.792	0.013	-0.107	0.013	-24.685
36JCM	325473	4175624	-24.751	0.016	-0.095	0.016	-24.656
37JCM	324695	4175940	-24.709	0.022	-0.085	0.022	-24.624
38JCM	323759	4176704	-24.642	0.025	-0.073	0.025	-24.569
39JCM	322233	4176270	-24.583	0.030	-0.061	0.030	-24.522
40JCM	321591	4176351	-24.560	0.032	-0.057	0.032	-24.503
LINE 9: SHERWIN CREEK-YMCA CAMP SPUR							
MGB13	332965	4167110	-24.844	0.021	-0.098	0.021	-24.746
11DOR	333018	4167142	-24.848	0.021	-0.099	0.021	-24.749
MGB10	333040	4166920	-24.837	0.023	-0.098	0.023	-24.739
MGB9	333286	4166859	-24.840	0.023	-0.098	0.024	-24.742
MGB8	333036	4166709	-24.827	0.022	-0.098	0.022	-24.729
MGB7	332983	4166677	-24.826	0.022	-0.099	0.022	-24.727
MGB6	332955	4166611	-24.822	0.022	-0.099	0.022	-24.723
LC1	332937	4166611	-24.822	0.022	-0.099	0.022	-24.723
MGB5	332937	4166589	-24.820	0.022	-0.099	0.021	-24.721
MGB4	332936	4166556	-24.819	0.022	-0.099	0.021	-24.72
MGB3	332909	4166523	-24.817	0.022	-0.099	0.022	-24.718
MGB2	332855	4166491	-24.814	0.022	-0.099	0.022	-24.715
MGB1	332728	4166316	-24.803	0.023	-0.099	0.023	-24.704
28EGE	332610	4166129	-24.792	0.024	-0.099	0.024	-24.693
LC2	332480	4165821	-24.774	0.024	-0.099	0.024	-24.675
29EGE	332256	4165670	-24.754	0.023	-0.096	0.023	-24.658
30EGE	332007	4165587	-24.746	0.024	-0.096	0.024	-24.65
LC3	331812	4165557	-24.741	0.025	-0.096	0.025	-24.645
LAKE CROWLEY TIE B							
1JD	340232	4166312	-24.934	0.028	-0.057	0.028	-24.877
48DOR	340225	4166867	-24.965	0.027	-0.065	0.026	-24.9
47DOR	340417	4168129	-25.026	0.020	-0.082	0.020	-24.944
46DOR	340781	4169143	-25.069	0.018	-0.095	0.018	-24.974
LC3E	342195	4168772	-25.071	0.022	-0.087	0.022	-24.984
LC3D	342979	4168734	-25.073	0.023	-0.083	0.023	-24.99
LC3C	344308	4169009	-25.079	0.023	-0.079	0.022	-25
LC3B	345492	4169542	-25.082	0.027	-0.078	0.027	-25.004
LC3A	345597	4168530	-25.055	0.029	-0.065	0.029	-24.99
TBM LC3	345623	4168529	-25.054	0.029	-0.064	0.029	-24.99

32 Converting NAD83 GPS Heights Into NAVD88 Elevations With LVGEOID, Long Valley Volcanic Region, California

Table 5. Geoid heights at leveling benchmarks for the Long Valley region (see fig. 1B for benchmark location)—Continued.

BM	UTM NAD27		LVGEOID (m)		Conversion surface s (m)		USGG2003
	X	Y	height	σ	height	σ	height (m)
LAKE CROWLEY TIE C							
1JD	340232	4166312	-24.934	0.028	-0.057	0.028	-24.877
LC2D	341542	4166475	-24.960	0.030	-0.054	0.030	-24.906
LC2C	342902	4166050	-24.956	0.031	-0.048	0.031	-24.908
LC2B	344414	4165710	-24.947	0.033	-0.036	0.033	-24.911
LC2A	345056	4164655	-24.903	0.033	-0.026	0.033	-24.877
TBM LC2	345054	4164533	-24.898	0.032	-0.026	0.032	-24.872
MARY LAKE ROAD							
J1383	325154	4168470	-24.714	0.026	-0.069	0.026	-24.645
CVO89-311	324483	4168018	-24.682	0.027	-0.056	0.027	-24.626
VISTA89	323772	4166990	-24.652	0.032	-0.052	0.032	-24.6
CVO89-310	323569	4166595	-24.646	0.032	-0.051	0.032	-24.595
CVO89-309	323181	4165770	-24.636	0.033	-0.050	0.034	-24.586
CVO89-308	323330	4164868	-24.621	0.035	-0.054	0.035	-24.567
CVO89-307	323397	4164289	-24.611	0.035	-0.055	0.036	-24.556
CVO89-306	323463	4164066	-24.607	0.035	-0.056	0.035	-24.551
CVO89-305	323529	4163854	-24.597	0.038	-0.056	0.038	-24.541
CVO89-304	323332	4163758	-24.596	0.038	-0.055	0.038	-24.541
CVO89-303	323171	4164072	-24.608	0.038	-0.053	0.038	-24.555
CVO89-302	322998	4164231	-24.613	0.038	-0.052	0.038	-24.561
CVO89-301	322516	4164397	-24.624	0.038	-0.048	0.038	-24.576
CVO89-300	321780	4164657	-24.638	0.037	-0.043	0.038	-24.595

¹ Experimental sites (see also table 2).

